

Manuscript Details

Manuscript number	IJBIOMAC_2018_7171_R2
Title	Structure of the capsular polysaccharide of the KPC-2-producing <i>Klebsiella pneumoniae</i> strain KK207-2 and assignment of the glycosyltransferases functions
Article type	Research Paper

Abstract

Klebsiella pneumoniae strain KK207-2 was isolated in 2010 from a bloodstream infection of an inpatient at an Italian hospital. It was previously found to produce the KPC-2 carbapenemase and to belong to clade 1 of sequence type 258. Genotyping of the conserved *wzi* and *wzc* genes from strain KK207-2 yielded contrasting results: the *wzc*-based method assigned the *cps*₂₀₇₋₂ to a new K-type, while the *wzi*-based method assigned it to the known K41 K-type. In order to resolve this contradiction, the capsular polysaccharide of *K. pneumoniae* KK207-2 was purified and its structure determined by using GLC-MS of appropriate carbohydrate derivatives, ESI-MS of both partial hydrolysis and Smith degradation derived oligosaccharides, and NMR spectroscopy of oligosaccharides, and the lithium degraded, native and de-O-acetylated polysaccharide. All the collected data demonstrated the following repeating unit for the *K. pneumoniae* KK207-2 capsular polysaccharide: OAc \square I 6 [3)- β -D-Gal-(1-4)- β -D-Glc-(1-]n 4 \square I 1 β -D-Glcp-(1-6)- α -D-Glcp-(1-4)- β -D-GlcpA-(1-6)- α -D-Glcp The polysaccharide contains about 0.60 acetyl groups per repeating unit on C6 of the Gal residue. The reactions catalysed by each glycosyltransferase in the *cps*_{KK207-2} gene cluster were assigned on the basis of structural homology with other *Klebsiella* K antigens.

Keywords	<i>Klebsiella pneumoniae</i> Sequence Type 258 strain KK207-2; capsular polysaccharide structure; glycosyltransferases
Manuscript category	Carbohydrates, Natural Polyacids and Lignins
Corresponding Author	Paola Cescutti
Order of Authors	Barbara Bellich, Neil Ravenscroft, Roberto Rizzo, Cristina Lagatolla, Marco D'Andrea, Gian Maria Rossolini, Paola Cescutti
Suggested reviewers	Joanna Kubler-Kielb, Kathryn E. Holt, Andrzej Gamian, Yuriy Knirel, Domenico Garozzo

Submission Files Included in this PDF

File Name [File Type]

Cover letter2.docx [Cover Letter]

Responses to Reviewers.docx [Response to Reviewers]

Abstract.docx [Abstract]

manuscript revised Cescutti_2.docx [Manuscript File]

Fig 1.pptx [Figure]

Fig 2.tif [Figure]

Fig 3.pptx [Figure]

Fig 4.pptx [Figure]

Fig 5.pptx [Figure]

Fig 6.pptx [Figure]

Fig 7.pptx [Figure]

Supplementary material 190218.pdf [e-Component]

To view all the submission files, including those not included in the PDF, click on the manuscript title on your EVISE Homepage, then click 'Download zip file'.

Dear Editor,

I carefully revised the manuscript according to the reviewers' comments. I accepted all their suggestions and changed the manuscript accordingly.

I also moved the "Materials and Methods" section before the "Results and discussion" one, as you suggested. I changed the numbering of the references accordingly, as well as those of Figs and Tables. Changes regarding the order of Figs and Tables were also made in the Supplementary file.

Thank you for your work

Regards

Paola

Responses to Reviewers

Reply to Reviewer 1

Thank you for all your comments and suggestions. I moved Table 1 to the supplementary material and numbered the remaining Tables accordingly, changed “Superdex G30” with “Superdex 30 prep grade” and checked all the DOI links.

Reply to Reviewer 2

Thank you for all your comments and suggestions. I inserted all suggested corrections in the text.

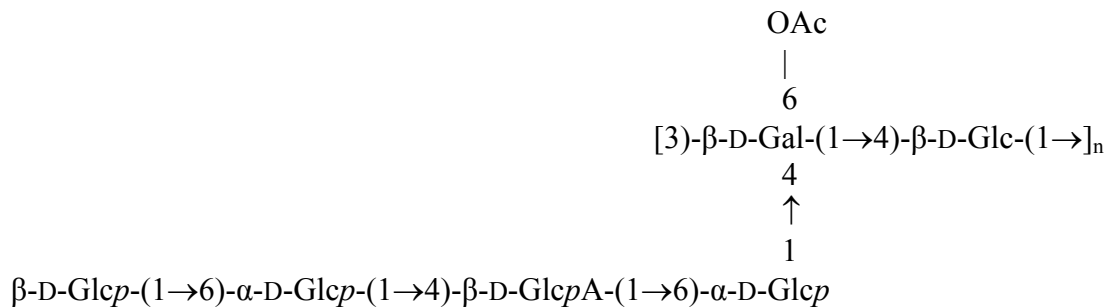
Regarding Fig 1, I forgot to “group” all the components of the figure, and for this reason there were no labels in it. Now I have corrected it. I also corrected the Figure legend by deleting “native **CPS KK207-2** (d)” whose ¹H NMR spectrum was not present in Fig. 1.

Regarding your comment: line 165, ...per-ethylated?

We used ethyl iodide to derivatise the sample in order not to have ambiguous results. In fact, the difference in mass between an Hex and an HexA is 14. The same mass value corresponds to substitution of an hydrogen atom with a methyl group. Using ethyl iodide this ambiguity is avoided.

Abstract

Klebsiella pneumoniae strain KK207-2 was isolated in 2010 from a bloodstream infection of an inpatient at an Italian hospital. It was previously found to produce the KPC-2 carbapenemase and to belong to clade 1 of sequence type 258. Genotyping of the conserved *wzi* and *wzc* genes from strain KK207-2 yielded contrasting results: the *wzc*-based method assigned the *cps*₂₀₇₋₂ to a new K-type, while the *wzi*-based method assigned it to the known K41 K-type. In order to resolve this contradiction, the capsular polysaccharide of *K. pneumoniae* KK207-2 was purified and its structure determined by using GLC-MS of appropriate carbohydrate derivatives, ESI-MS of both partial hydrolysis and Smith degradation derived oligosaccharides, and NMR spectroscopy of oligosaccharides, and the lithium degraded, native and de-O-acetylated polysaccharide. All the collected data demonstrated the following repeating unit for the *K. pneumoniae* KK207-2 capsular polysaccharide:



The polysaccharide contains about 0.60 acetyl groups per repeating unit on C6 of the Gal residue. The reactions catalysed by each glycosyltransferase in the *cps*_{KK207-2} gene cluster were assigned on the basis of structural homology with other *Klebsiella* K antigens.

1
2
3 **Structure of the capsular polysaccharide of the KPC-2-producing *Klebsiella pneumoniae***
4 **strain KK207-2 and assignment of the glycosyltransferases functions**
5
6

7 Barbara Bellich^a, Neil Ravenscroft^b, Roberto Rizzo^a, Cristina Lagatolla^a, Marco Maria D'Andrea^{c,d}
8 Gian Maria Rossolini^{e,f} and Paola Cescutti^{a*}
9

10
11
12 ^a Department of Life Sciences, University of Trieste, via L. Giorgieri 1, Bdg C11, 34127 Trieste,
13 Italy
14

15 ^b Department of Chemistry, University of Cape Town, Rondebosch 7701, South Africa

16 ^c Department of Medical Biotechnologies, University of Siena, Siena, Italy

17 ^d Department of Biology, University of Rome "Tor Vergata", Rome, Italy

18 ^e Department of Experimental and Clinical Medicine, University of Florence, Florence, Italy

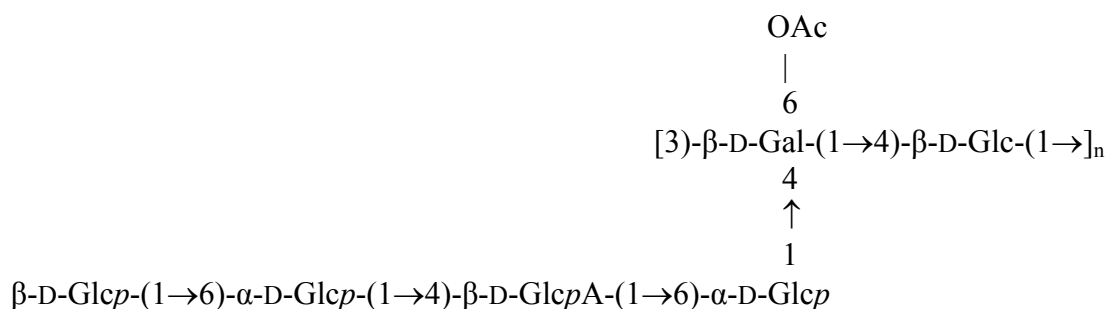
19 ^f Microbiology and Virology Unit, Florence Careggi University Hospital, Florence, Italy
20
21
22
23

24
25 Corresponding author at: Department of Life Sciences, University of Trieste, via L. Giorgieri 1,
26 Bdg C11, 34127 Trieste, Italy.
27

28 *E-mail address:* pcescutti@units.it (Paola Cescutti)
29
30
31
32
33
34
35
36
37
38
39
40
41
42
43
44
45
46
47
48
49
50
51
52
53
54
55
56
57
58
59

60
61 **Abstract**
62
63

64 *Klebsiella pneumoniae* strain KK207-2 was isolated in 2010 from a bloodstream infection of an
65 inpatient at an Italian hospital. It was previously found to produce the KPC-2 carbapenemase and to
66 belong to clade 1 of sequence type 258. Genotyping of the conserved *wzi* and *wzc* genes from strain
67 KK207-2 yielded contrasting results: the *wzc*-based method assigned the *cps*₂₀₇₋₂ to a new K-type,
68 while the *wzi*-based method assigned it to the known K41 K-type. In order to resolve this
69 contradiction, the capsular polysaccharide of *K. pneumoniae* KK207-2 was purified and its structure
70 determined by using GLC-MS of appropriate carbohydrate derivatives, ESI-MS of both partial
71 hydrolysis and Smith degradation derived oligosaccharides, and NMR spectroscopy of
72 oligosaccharides, and the lithium degraded, native and de-O-acetylated polysaccharide. All the
73 collected data demonstrated the following repeating unit for the *K. pneumoniae* KK207-2 capsular
74 polysaccharide:
75
76
77
78
79
80
81



92 The polysaccharide contains about 0.60 acetyl groups per repeating unit on C6 of the Gal residue.
93 The reactions catalysed by each glycosyltransferase in the *cps*_{KK207-2} gene cluster were assigned on
94 the basis of structural homology with other *Klebsiella* K antigens.
95
96
97
98
99

100 **Keywords:** *Klebsiella pneumoniae* Sequence Type 258; strain KK207-2; capsular polysaccharide
101 structure; NMR; ESI-MS; glycosyltransferases.
102
103
104
105
106
107
108
109
110
111
112
113
114
115
116
117
118

1. Introduction

Klebsiella pneumoniae is a Gram-negative encapsulated rod which is mostly responsible for nosocomial infections in immunocompromised patients, but can also cause severe community-acquired infections [1]. The clinical scenario has worsened during recent years, with the global emergence and dissemination of *K. pneumoniae* strains resistant to carbapenems (CR-Kp), which are among the last-resort antibiotics for treatment of infections caused by multiresistant Gram-negative rods. Production of carbapenemase of different types (e. g. KPC, VIM, NDM, OXA-48) is the major carbapenem resistance mechanism among CR-Kp. KPC-type carbapenemases are among the most prevalent and challenging carbapenemases, since they can degrade virtually all β -lactam antibiotics including carbapenems [2]. Dissemination of KPC-producing strains of *K. pneumoniae* (KPC-Kp) has been sustained by the expansion of various clones, with members of clonal group (CG) 258 being likely the most successful and widespread. CG258 includes strains of the sequence type (ST) 258 and some related variants [2]. Infections caused by KPC-Kp strains are challenging in healthcare settings, where they spread rapidly and are associated with significant morbidity and mortality [2].

K. pneumoniae strains can be classified based on serotyping of two different types of antigens exposed on the bacterial surface: O antigen, the outer polysaccharide chain of the lipopolysaccharide, and the K antigen, the capsule. *K. pneumoniae* produces approximately 80 structurally different capsular polysaccharides (CPS, or K antigen) which are recognized as virulence factors and confer different antigenic properties within the same species, with relevant consequences to bacterial virulence. Although serotyping of K antigen has been extensively used to classify *K. pneumoniae* strains, genotyping of the conserved *wzi* [3] and *wzc* [4] genes has recently been developed to establish the K-type. Moreover, Pan *et al.* [5] carried out an extended analysis of the sequences of the *cps* clusters from strains belonging to 79 different K types, identifying more than 1500 different genes that were grouped into 361 homology groups. Despite this high number of different CPSs expressed by *K. pneumoniae* strains, capsular variations are limited among KPC-Kp isolates, due to their clonal origin.

Genotyping of KPC-Kp isolates belonging to ST258 [6, 7] identified the presence of at least two lineages, indicated as clade I and clade II, which differ from each other primarily in the *cps* gene cluster (named *cps-1* and *cps-2* gene cluster, respectively) and are novel with respect to those described by Pan *et al* [5]. Regarding *cps-1*, the results obtained with the two genotyping methods were not in agreement with each other: the *wzc*-based method [4] assigned *cps-1* to a new K-type, while the *wzi*-based method [3] associated it to the already known K41 K-type. However, the *cps-1*

178
179 cluster does not contain the genes for the biosynthesis of rhamnose, thus suggesting a chemical
180 structure at least partially different from K41.
181

182 The present work reports the primary structure of the CPS produced by *K. pneumoniae* KK207-2
183 [6], a clade I representative, determined by using GLC-MS of appropriate carbohydrate derivatives,
184 ESI-MS of both partial hydrolysis and Smith degradation derived oligosaccharides, and NMR
185 spectroscopy of oligosaccharides, lithium degraded CPS, and the native and de-O-acetylated CPS.
186
187 Moreover, taking advantage of the sequenced *cps*₂₀₇₋₂ gene cluster [6], and of the structural
188 knowledge gained in the present investigation, each glycosyltransferase (GT) in the CPS gene
189 cluster was assigned to the corresponding catalyzed reaction.
190
191
192
193
194

195 **2. Materials and methods**

196 197 198 *2.1. Bacterial strain, capsular polysaccharide production and purification*

199
200
201 The strain of *Klebsiella pneumoniae* KK207-2 was isolated in 2010 from a bloodstream
202 infection of an inpatient at an Italian hospital, and was previously described to produce the KPC-2
203 carbapenemase and to belong to ST258 [6]. Bacterial cells were grown on 25 Worfel-Ferguson agar
204 plates for 4 days at 30°C. The bacterial lawn was collected with 0.9 % NaCl (about 3 mL per dish),
205 gently stirred at 10 °C for 2 h, centrifuged at 22400 x g at 4 °C for 30 min to separate the cells from
206 the supernatant which was precipitated with 4 vol of cold ethanol. The precipitated material was
207 recovered by centrifugation at 1900 x g at 4 °C for 30 min, dissolved in water, dialyzed first against
208 0.1 M NaCl and then water, taken to pH = 6.9, filtered (Millipore membranes 0.45 µm) and
209 lyophilized. The bacterial cells recovered in the pellet of the first centrifugation were suspended in a
210 2% phenol solution at 10 °C for 2 h, centrifuged at 22400 x g at 4 °C for 30 min and the supernatant
211 was treated as the one reported above. The purified capsular polysaccharide was named **CPS**
212
213
214
215
216
217
218
219 **KK207-2**.

220 221 222 *2.2. General procedures*

223
224
225 Native and permethylated oligo- and polysaccharides were hydrolysed with 2 M trifluoroacetic
226 acid (TFA) at 125 °C for 1 h. Alditol acetates were prepared as previously described [8]. TMS
227 methyl glycosides were obtained by derivatization with the reagent Sylon™ HTP (Sigma) after
228 methanolysis of the polysaccharide [9]. In order to detect the possible presence of uronic acids,
229 different methanolysis procedures were applied using 2 M HCl in methanol: i) at 85 °C for 16 h; ii)
230
231
232
233
234
235
236

237
238 hydrolysis with 2 M TFA at 100 °C for 1 h, followed by methanolysis at 85 °C for 16 h; iii) at 121
239 °C for 5 min and iv) at 121 °C for 15 min in a microwave oven (CEM- Discover® SP Microwave).
240
241 Permethylation of the CPS and oligosaccharides was achieved following the protocol by Harris
242 [10]. Integration values of the areas of the partially methylated alditol acetates (PMAA) were
243 [10]. Integration values of the areas of the partially methylated alditol acetates (PMAA) were
244 corrected by the effective carbon response factors [11]. De-O-acetylation was obtained by stirring
245 the CPS (100 mg) in 10 mM NaOH (1 mg/mL) for 5 h under a stream of nitrogen. Carboxyl
246 reduction was performed on 20 mg of CPS using carbodiimide [12] and following the modification
247 described by Osman *et al.*[13]. Size exclusion chromatography of **deOAc CPS KK207-2** was
248 performed on a Sephacryl S-400 column (1.6 cm i.d. × 90 cm) using 0.05 M NaNO₃ as eluent, and a
249 flow rate of 7.2 mL/h. Fractions were collected at 15 min intervals. Elution was monitored using a
250 refractive index detector (Knauer, RI detector K-2301, Lab-Service Analytica) which was interfaced
251 with a computer via PicoLog software. The head, core and tail fractions of the eluted peak were
252 pooled together, dialyzed and used for ¹H NMR spectroscopy.
253
254
255
256
257
258

259 Oligosaccharides were separated on a Bio Gel P2 column (1.6 cm i.d. x 90 cm) using the same
260 conditions and set up reported above, except the collection of fractions performed at 12 min
261 interval.
262

263 Oligosaccharides were desalted on a Superdex 30 prep grade column (1.0 cm i.d. x 82 cm)
264 using water as eluent at a flow rate of 1.5 mL/min. Elution was monitored using a refractive index
265 detector (Knauer, RI detector Smartline 2300, Lab-Service Analytica) which was interfaced with a
266 computer via Clarity software. Fractions were collected at 30 sec interval.
267
268
269

270 Analytical GLC was performed on a Perkin-Elmer Autosystem XL gas chromatograph
271 equipped with a flame ionization detector and using He as carrier gas. An HP-1 capillary column
272 (Agilent Technologies, 30 m) was used to separate alditol acetates (temperature program: 3 min at
273 150 °C, 150–270 °C at 3 °C/min, 2 min at 270 °C), PMAA (temperature program: 1 min at 125 °C,
274 125–240 °C at 4 °C/min, 2 min at 240 °C), TMS methyl glycosides (temperature program: 1 min at
275 150 °C, 150–280 °C at 3 °C/min, 2 min at 280 °C), and TMS (+)-2-butyl glycosides, for the
276 determination of the absolute configuration of the sugar residues [14], (temperature program: 1 min
277 at 50 °C, 50-130 °C at 45 °C/min, 1 min at 130 °C, 130–200 °C at 1 °C/min, 10 min at 200 °C).
278
279
280
281
282
283
284
285
286
287
288
289
290
291
292
293
294
295

2.3. Partial acid hydrolysis of the **deOAc CPS KK207-2**, purification and characterization of the oligosaccharides obtained

296
297 **deOAc CPS KK207-2** (33 mg) was hydrolyzed with 32 mL of 0.5 M TFA at 100 °C for 2 h.
298
299 The sample was roto-evaporated to dryness under reduced pressure, followed by three washes with
300 water. After dissolution in 10 mL of water, the sample was taken to pH = 6.8, and recovered by
301 lyophilization. Separation of the products was achieved by size-exclusion chromatography on a Bio
302 Gel P2 column with a flow rate of 6.8 mL/h. Fractions belonging to the same peak were pooled
303 together and desalted on a Superdex 30 prep grade column. De-salted homogenous fractions were
304 combined after determining their composition by ESI-MS, and structurally characterized by ESI-
305 MS, NMR spectroscopy and GLC-MS of the PMAA derivatives.
306
307
308
309

310
311
312 *2.4. Smith degradation of the **deOAc CPS KK207-2**, purification and characterization of the*
313 *oligosaccharides obtained*
314

315
316 **deOAc CPS KK207-2** was subjected to Smith degradation [15]: 33 mg of the polysaccharide
317 were dissolved in 6 mL of water, 0.7 mL of a 0.29 M NaIO₄ solution were added (0.8 moles of
318 NaIO₄/1 mole of oxidizable diol) and the oxidation was let to proceed for 1 h in the dark at 10 °C.
319 After addition of glycerol to react with excess of periodate, reduction of the aldehyde groups was
320 achieved by incubation with NaBH₄ at room temperature for 16 h. Excess of borohydride was
321 destroyed with 50% aqueous acetic acid and the solution was dialyzed. The recovered material was
322 hydrolysed with 0.5 M TFA for 6 days at room temperature, rotoevaporated to dryness, washed
323 three times with water to remove TFA, taken to pH = 7.0 and recovered by lyophilization. The
324 products were separated on a Bio Gel P2 column with a flow rate of 7.2 mL/h. Fractions belonging
325 to the same peak were pooled together and desalted on a Superdex 30 prep grade column. De-salted
326 homogenous fractions were combined after determining their composition by ESI-MS, and
327 structurally characterized by ESI-MS, NMR spectroscopy and GLC-MS of the PMAA derivatives.
328
329
330
331
332
333
334
335
336

337 *2.5. Lithium degradation of the **CPS KK207-2**, purification and characterization of the products*
338 *obtained*
339
340

341
342 **CPS KK207-2** was subjected to degradation with lithium metal following the protocol by Lau et
343 al. [16]. The CPS (20 mg) was dissolved in 4 mL of ethylenediamine and treated with lithium wire;
344 it was then purified according to literature procedures [16], except that the resin used was Amberlite
345 IR H⁺120. After the ion exchange procedure, the sample was lyophilized and separated by size
346 exclusion chromatography on a Bio Gel P2 column (Fig. S1). The peak eluting at the exclusion
347
348
349
350
351
352
353
354

355
356 volume of the column was dialyzed (Spectra Por 6 membrane, CO 1000 Da), and recovered by
357 freeze-drying.
358
359

360 361 2.6. ESI mass spectrometry 362 363

364 ESI mass spectra were recorded on a Bruker Esquire 4000 ion trap mass spectrometer connected
365 to a syringe pump for the injection of the samples. The instrument was calibrated using a tune
366 mixture provided by Bruker. Oligosaccharides were dissolved in 50% aqueous methanol - 11 mM
367 NH₄OAc; permethylated oligosaccharides were dissolved in a 1:1 chloroform : methanol mixture,
368 11mM NH₄OAc. Samples were injected at 180 μ L/h. Detection was performed in the positive ion
369 mode.
370
371
372
373
374

375 2.7. NMR experiments 376 377

378 The **CPS KK207-2** and **deOAc CPS KK207-2** samples were dissolved in water (about 3
379 mg/mL) and sonicated using a Branson sonifier equipped with a microtip at 2.8 Å, in order to
380 decrease their molecular masses. The samples were cooled in an ice bath and sonicated using 10
381 bursts of 1 min each, separated by 1 min intervals. The polysaccharides (~5 mg) were exchanged
382 twice with 99.9% D₂O by lyophilization and then dissolved in 0.6 mL of 99.96% D₂O and
383 introduced into a 5 mm NMR tube for data acquisition. 1D ¹H and ¹³C and 2D, COSY, TOCSY,
384 NOESY, HSQC, HMBC and hybrid HSQC-TOCSY and HSQC-NOESY spectra were obtained
385 using a Bruker Advance III 600 MHz NMR spectrometer equipped with a BBO Prodigy cryoprobe
386 and processed using standard Bruker software (Topspin 3.2). The probe temperature was set at 343
387 K. 2D TOCSY experiments were performed using mixing times of 180 ms and the 1D variants
388 using mixing times up to 200 ms. The 2D NOESY experiment and 1D variants were performed
389 using a mixing time of 300 ms. The HSQC (with multiplicity editing) experiment was optimized for
390 J = 145 Hz (for directly attached ¹H-¹³C correlations), and the HMBC experiment optimized for a
391 coupling constant of 8 Hz (for long-range ¹H-¹³C correlations). HSQC-TOCSY and HSQC-NOESY
392 NMR spectra were recorded using mixing times of 120 and 300 ms, respectively. 2D experiments
393 were recorded using non-uniform sampling: 50% for homonuclear and 25% for heteronuclear
394 experiments. Spectra were referenced relative to H-2/C-2 of β -Glc: ¹H at 3.34 ppm and ¹³C at 74.0
395 ppm, established using acetone as an internal standard.
396
397
398
399
400
401
402
403
404
405
406

407 Oligosaccharides were exchanged twice with 99.9% D₂O by lyophilization and then dissolved in
408 0.6 mL of 99.96% D₂O. Spectra were recorded on a 500 MHz Varian spectrometer operating at 333
409
410
411
412
413

414
415 K. 2D experiments were performed using standard pulse sequences and pulsed field gradients for
416 coherence selection when appropriate. HSQC spectra were recorded using 145 Hz (for directly
417 attached ^1H - ^{13}C correlations). TOCSY spectra were acquired using 150 ms spin-lock time and a 1.2
418 s relaxation time. NOESY experiments were recorded with 200 ms mixing time and a 1.2 s
419 relaxation time. NMR spectra were processed using MestreNova software. Chemical shifts are
420 expressed in ppm using acetone as internal reference (2.225 ppm for ^1H and 31.07 ppm for ^{13}C).
421
422
423
424
425

426 **3. Results and Discussion**

427

428 *3.1. Purification and composition analysis of CPS KK207-2*

429
430
431

432
433 The strain *Klebsiella pneumoniae* KK207-2 was grown on carbohydrate rich Worfel-Ferguson
434 agar medium for 4 days at 30°C. The bacterial lawn was first collected with 0.9 % NaCl and
435 subsequent purification gave 224 mg of polysaccharide, while treatment of the remaining bacterial
436 cells with a 2% phenol solution followed by purification resulted in 152 mg of polysaccharide. ^1H
437 NMR spectroscopy showed that the two samples were identical and the polysaccharide was named
438 **CPS KK207-2**. ^1H NMR spectroscopy determined about 0.60 O-acetyl groups per repeating unit.
439 An aliquot of de-acetylated sample (**deOAc CPS KK207-2**) eluted as a single broad peak upon size
440 exclusion chromatography on a Sephacryl S-400 column (data not shown); the head, core and tail
441 fractions of the peak were pooled and analyzed by ^1H NMR spectroscopy which showed that the
442 three fractions were structurally homogenous, indicating the production of a single polysaccharide.
443
444
445
446
447
448

449 Composition analysis as alditol acetate derivatives revealed Gal and Glc in the molar ratios 1.0
450 : 2.5, while analysis of methyl-glycosides trimethylsilyl (TMS) derivatives confirmed Gal and Glc
451 in variable molar ratios depending on the experimental conditions used (from 1.0 : 3.1 to 1.0 : 5.3),
452 but did not reveal the presence of any uronic acids. The position of the glycosidic linkages was
453 determined by GLC and GLC-MS analysis after derivatization of the sugar components to partially
454 methylated alditol acetates. GLC analysis on a HP-1 column showed four peaks attributed to t-Glc,
455 4-linked Glc, 6-linked Glc and 3,4-linked Gal, all in the pyranose configuration. Integration of the
456 respective peak areas, after correction for the effective carbon response factors [11], gave the
457 relative molar ratios reported in Table S1. In order to verify the presence of uronic acids, **CPS**
458 **KK207-2** was reduced with carbodiimide [12,13], and linkage analysis revealed double the amount
459 of 4-linked Glc (Table S1), thus indicating a 4-linked Glc_pA residue in the native CPS. These data
460 also showed that **CPS KK207-2** has a branched repeating unit made of six monosaccharides. The
461 absolute configuration was established to be D for all residues.
462
463
464
465
466
467
468
469
470
471
472

473
474
475
476 *3.2. Production and characterization of the oligosaccharides obtained by partial acid hydrolysis of*
477 *deOAc CPS KK207-2*
478

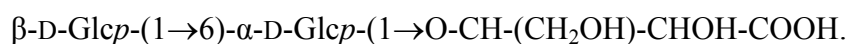
479
480 **deOAc CPS KK207-2** was treated with 0.5 M TFA and the products were separated by size
481 exclusion chromatography on a Bio Gel P2 column. The elution profile is reported in Fig. S2a.
482 Fractions belonging to the same peak were pooled together and, after desalting, subjected to ESI-
483 MS and ¹H NMR spectroscopy to identify peaks suitable for further structural investigation. The
484 partial hydrolysis treatment gave only one reasonably pure peak (**PH-2**) which was identified by
485 ESI-MS as the disaccharide HexA-Hex; only 6-linked Glc was detected by GLC-MS analysis of the
486 PMAA derivatives. The ¹H NMR spectrum (Fig. 1a) gave the three signals in the anomeric region at
487 5.23, 4.65 and 4.50 ppm (with integration values of 0.3, 0.5, and 1.0, respectively), assigned to H-1
488 of the reducing end 6-Glc- α and 6-Glc- β , and of t-GlcpA- β , respectively, thus identifying **PH-2** as
489 the aldobiuronic acid β -D-GlcpA-(1 \rightarrow 6)-D-Glc-OH.
490
491
492
493
494
495
496
497

498 *3.3. Production and characterization of the oligosaccharides obtained by Smith degradation of*
499 *deOAc CPS KK207-2*
500
501
502

503 **deOAc CPS KK207-2** was subjected to partial periodate oxidation, because, due to the type of
504 glycosidic linkages, a complete oxidation would have left only the branched Gal residue intact,
505 resulting in little structural information. After oxidation, the sample was subjected to Smith
506 degradation [15] and the oligosaccharides produced separated by size exclusion chromatography on
507 a Bio Gel P2 column (Fig. S2b). Fractions belonging to the same peak were pooled together,
508 desalted and subjected to ESI-MS and ¹H NMR spectroscopy to identify peaks containing mainly
509 only one oligosaccharide and thus suitable for further structural investigation. In this way two peaks
510 were selected, named **SD-1** and **SD-2**.
511
512
513
514

515
516 The most intense ion in the ESI mass spectrum of the sample **SD-2** (Fig. 2a) at 483.2 *m/z*
517 corresponded to the sodium adduct of a compound constituted of two hexoses and one 2,3,4-
518 trihydroxybutanoic acid (THBA) moiety at the reducing end, the latter deriving from oxidation of
519 the 4-linked GlcA residue. MS² of the ion at 483.2 *m/z* (Fig. 2b) gave the sequence Hex-Hex-
520 THBA. A less intense ion at 637.2 *m/z* was present in the ESI mass spectrum (data not shown) and
521 it was attributed to the oligosaccharide found as main component in **SD-1** (see next paragraph). **SD-**
522 **2** was per-methylated and subjected to ESI-MS and MS² which confirmed both its composition and
523 sequence. After hydrolysis and derivatization to alditol acetates, GLC-MS analysis showed t-Glc
524
525
526
527
528
529
530
531

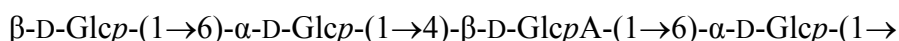
532
533 and 6-Glc in the relative molar ratio 1.0 : 0.8. The ¹H NMR spectrum (Fig. 1b) gave three signals in
534 the anomeric region: two resonances at 5.15 and 4.48 ppm (with integration values of 1.0, and 1.6,
535 respectively), were attributed to H-1 of 6-linked α-D-Glcp and t-β-D-Glcp respectively, while the
536 less intense signal at 5.47 ppm, with integration value of 0.3, was assigned to a residue in the
537 oligosaccharide **SD-1** (Fig. 1c), in agreement with ESI-MS data. Homo- and hetero-nuclear 2D
538 NMR experiments (data not shown) gave all the chemical shifts for each spin system (Table S2) and
539 established the following structure:
540



541 The residue α-D-Glcp is linked to C3 of the THBA, as expected for a 4-linked GlcpA.
542 ESI-MS of the oligosaccharides **SD-1** (Fig. 2c) indicated two hexoses and a hexuronic acid with
543 glycerol at the reducing end; MS² of the ion at 615.1 *m/z* (Fig. 2d) gave the sequence Hex-Hex-
544 HexA-Gro. The sample was per-ethylated and subjected to ESI-MS and MS² which confirmed both
545 the composition and the sequence. After hydrolysis and derivatization to alditol acetates, GLC-MS
546 identified two main peaks with t-Glc and 6-Glc in the relative molar ratio 1.0 : 1.7. The ¹H NMR
547 spectrum (Fig. 1c) contained two anomeric signals at 5.47 and 4.49 ppm, the latter with integration
548 values corresponding to two residues. Based on the chemical shifts assignments for **PH-2** and **SD-2**,
549 and on the 2D NMR data, the signal at 5.47 ppm was attributed to α-D-Glcp, and those at 4.49 ppm
550 to β-D-GlcpA and β-D-Glcp. Homo- and hetero-nuclear 2D NMR experiments (data not shown)
551 determined the chemical shifts for each spin system (Table S3). NOESY plot showed inter-residue
552 connectivities between H-1 (4.49 ppm) of t-β-D-Glcp to H-6 (3.89 ppm) of 6-linked α-D-Glcp, and
553 H-1 (5.47 ppm) of 6-linked α-D-Glcp to H-4 (3.81 ppm) of 4-linked β-D-GlcpA, thus establishing
554 the following structure β-D-Glcp-(1→6)-α-D-Glcp-(1→4)-β-D-GlcpA-(1→1)-Gro, in agreement
555 with ESI-MS data. The deshielded chemical shift of Gro C-1 at 71.93 ppm is due to its linkage to C-
556 1 of β-D-GlcpA, thus indicating that the uronic acid is linked to C-6 of another 6-linked α-D-Glcp in
557 the CPS.
558

559 The fractions eluted in the void volume of the Bio Gel P2 column (**SD-Vo**) were subjected to
560 linkage analysis and the results (Table S1) showed a significant change in the relative molar ratios
561 with the additional presence of 3-linked Gal, deriving from the original 3,4-linked Gal. By
562 calculating the molar ratios relative to the sum of the values for 3-linked Gal and 3,4-linked Gal,
563 since only this residue is not susceptible to oxidation (column IV, Table S1), it was clear that 4-Glc
564 had not been oxidised, whereas about half of the branched galactose had become 3-linked Gal,
565 suggesting that the side chain is linked to C-4 of the Gal residue.
566

567 The experimental findings obtained from analyzing the Smith degradation products suggested
568 that **CPS KK207-2** has a disaccharide backbone and the following side chain:
569



595
596 **3.4. NMR assignments for CPS KK207-2 repeating unit**
597

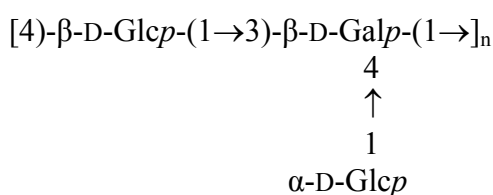
598
599 The repeating unit (RU) structure of **deOAc CPS KK207-2** was investigated at 600 MHz. The
600 ¹H NMR spectrum contains six main anomeric signals designated **A** to **F** (Fig. 1d). Residues **A** and
601 **E** gave sharp peaks at 5.48 and 4.49 ppm and resulted in strong crosspeaks in the 2D experiments;
602 these were attributed to the flexible terminal disaccharide β -D-Glcp-(1→6)- α -D-Glcp-(1→
603 identified in **SD-1**. The remaining residues gave broad anomeric signals and 2D crosspeaks of lower
604 intensity characteristic of units with restricted motion and branch points. The hexasaccharide RU
605 spin systems were elucidated using a combination of 1D and 2D ¹H-¹H correlation experiments with
606 correlations established from the six anomeric protons. The anomeric region of COSY, shown as an
607 overlay with TOCSY (Fig. 3), gave H-1 to H-2 for each residue. TOCSY (180 ms) gave additional
608 correlations for each of the spin systems depending on the coupling constants: H-1 to H-6 for α -Glc
609 (residue **A** at 5.48 ppm) and β -Glc (residues **C** and **E** at 4.69 and 4.49 ppm), H-1 to H-4 for α -Glc
610 (residue **B** at 4.92 ppm) and β -GlcA (residue **F** at 4.48 ppm), and H-1 to H-3 for β -Gal (residue **D** at
611 4.59 ppm). These assignments were confirmed and additional correlations established using 1D
612 TOCSY experiments recorded using a mixing time of 200 ms (Fig. S3): H-1 to H-4 for residue **D**
613 (β -Gal), H-1 to H-5 for residue **F** (β -GlcA) and H-1 to H-6 for residue **B** (α -Glc). Through-space
614 correlations, indicated by negative peaks in the 1D TOCSY spectra, were revealed in the anomeric
615 region of the NOESY experiment (Fig. 4). NOESY (300 ms) gave intra-residue correlations, mainly
616 H-1 to H-2 for the α -sugars and H-1 to H-3 and H-5 for the β -sugars including the 3,4-linked β -Gal
617 (**D**). NOESY also gave inter-residue correlations to the neighbouring residue and the linkage site
618 proton for most units: H-1 α -Glc (**A**) to H-4 of GlcA (**F**), H-1 α -Glc (**B**) to H-5 of β -Gal (**D**), H-1
619 β -Glc (**C**) to H-3 (and H-5) of β -Gal (**D**), H-1 β -Gal (**D**) to H-4 of β -Glc (**C**), and H-1 β -Glc (**E**) to
620 H-6 and H-6' of α -Glc (**A**). Small crosspeaks were detected at a lower level between H-1 α -Glc (**B**)
621 to H-4 of β -Gal (**D**) at 4.27 ppm and H-1 β -GlcA (**F**) to H-6' of α -Glc (**B**) at 3.95 ppm, thus
622 elucidating all the linkage positions in the **CPS KK207-2** RU. The assignments and sequence of
623 residues in the RU were corroborated by ¹H-¹³C correlation experiments: edHSQC, HSQC-TOCSY,
624 HSQC-NOESY and HMBC. This permitted full assignment of the ¹H and ¹³C chemical shifts for
625 each spin system which are collected in Table 1 and the ¹³C assignments are shown in Fig. 5.
626 Downfield displacements of the signals for C-6 of **A** and **B**, C-4 of **C** and C-3 and C-4 of **D**
627 compared to their shifts in the spectra of the corresponding non-substituted monosaccharides [17],
628 demonstrated the glycosylation pattern of the RU. This was in agreement with the NOESY data and
629
630
631
632
633
634
635
636
637
638
639
640
641
642
643
644
645
646
647
648
649

confirmed by inter-residue ^1H and ^{13}C correlations established using HMBC and HSQC-NOESY. Some key HMBC correlations are shown in Fig. 6, displayed as an overlay with HSQC: H-1 of α -Glc (**A**) to C-4 of GlcA (**F**) at 77.4 ppm, H-1 of β -Glc (**C**) to C-3 of β -Gal (**D**) at 82.0 ppm, H-1 β -Glc (**E**) to C-6 of α -Glc (**A**) at 68.7 ppm and H-4 of β -Gal (**D**) to C-1 of α -Glc (**B**) at 99.5 ppm. Thus a combination of ^1H - ^1H and ^1H - ^{13}C experiments confirmed the linkage positions, sequence and structure of the hexasaccharide RU with the main chain disaccharide $\rightarrow 4$)- β -D-Glc-(1 \rightarrow 3)- β -D-Gal-(1 \rightarrow and the tetrasaccharide side chain β -D-Glc-(1 \rightarrow 6)- α -D-Glc-(1 \rightarrow 4)- β -D-GlcA-(1 \rightarrow 6)- α -D-Glc \rightarrow linked to C-4 of β -D-Gal.

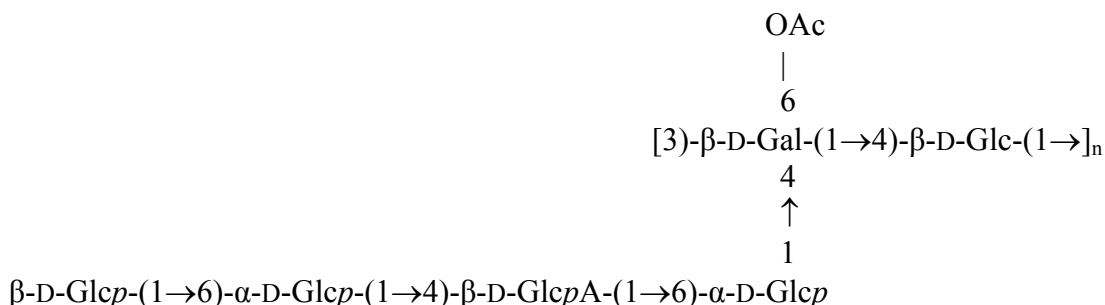
The ^1H NMR spectrum of native **CPS KK207-2** contains a singlet at 2.16 ppm due to \sim 60% O-acetylation. 2D NMR experiments identified that the O-acetylation was on a single site: C-6 of the 3,4-linked β -D-Gal (unit **D**). Comparison of the HSQC spectra for **deOAc CPS KK207-2** and **CPS KK207-2** showed a decrease in the intensity of the C-6 Gal peak at 61.0 ppm and the presence of a new peak at 63.6 ppm with attached protons at 4.35 and 4.36 ppm attributed to the CH_2OAc group of β -D-Gal6Ac.

3.5. Characterization of the products obtained by lithium degradation of the **CPS KK207-2**

CPS KK207-2 was treated with lithium metal [16], in order to destroy the glucuronic acid residue, and subsequently purified on a Bio Gel P2 column; the elution profile is shown in Fig. S1. The fractions eluting in the void volume of the column, were grouped and named **Li CPS KK207-2** were subjected to 1D and 2D NMR spectroscopy in order to confirm the sequence in the polysaccharide backbone. The ^1H NMR spectrum (Fig. 1e) showed three main anomeric signals at 4.97, 4.71, and 4.56 ppm, which were assigned to t- α -Glc, 4-linked β -Glc and 3,4-linked β -Gal, respectively, based on previous findings. A less intense signal at 4.49 ppm was attributed to residual GlcA which had not been destroyed completely by the lithium treatment. Homo- and heteronuclear 2D NMR experiments (data not shown) determined the chemical shifts for each spin system (Table S4). Some key HMBC correlations are shown in Fig. S4, displayed as an overlay with HSQC: H-1 of α -Glc to C-4 of β -Gal at 76.63 ppm, H-1 of β -Glc to C-3 of β -Gal at 81.62 ppm, and H-1 β -Gal to C-4 of β -Glc at 80.16 ppm. These inter-residue correlations confirmed the linkages and sequence resulting in the following repeating unit structure:



In conclusion, all the experimental data collected demonstrated that the capsular polysaccharide produced by *Klebsiella pneumoniae* clinical strain KK207-2, belonging to the sequence type ST258, has a repeating unit comprised of a disaccharide backbone and a tetrasaccharide side chain, with the following structure:



This structure is a novel one among the *K. pneumoniae* K antigens, in agreement with the original structure of the *cps*₂₀₇₋₂ gene cluster based on the *wzc*-based genotyping method [4,6]. **CPS KK207-2** shares structural similarities with other K antigens. In fact, it has the same backbone of K22 [18], including the O-acetyl position on C-6 of the Gal residue, K25 [19], and K37 [20]. Furthermore, part of its side chain is also present in K18 [21], K22, K23 [22], K26 [23], K37 and K41 [24] polysaccharides (Fig. S5).

3.6. Prediction of the reactions catalyzed by the *cps*₂₀₇₋₂ gene cluster glycosyltransferases

Taking advantage of the sequenced *cps*₂₀₇₋₂ gene cluster [6], and of the structural knowledge gained in the present investigation, the assignment of each glycosyltransferase (GT) to the corresponding catalyzed reaction was undertaken. The *cps* gene cluster in *Klebsiella* consists of some highly conserved genes together with a less conserved region [5]. Among the highly conserved are six genes located at the 5' end and mainly involved in the export and polymerization of the repeating unit (*galF*, *cpsACP*, *wzi*, *wza*, *wzb*, *wzc*), and two genes located at the 3' end and encoding for glucose-6-phosphate dehydrogenase and UDP-glucose dehydrogenase (*gnd* and *ugd*). The central region is the less conserved one and is responsible for K-type variation. In the *cps*₂₀₇₋₂ cluster such region contains mainly genes coding for GTs. The structural similarity of **CPS KK207-2** with K22 [18] and K37 [20] polysaccharides agrees with the high homology detected within their corresponding *cps* gene clusters [6]. In fact, the gene content of *cps*₂₀₇₋₂ is the same of *cps*_{K22} except for a transposon insertion that caused the substitution of three genes in the central region of the cluster. *cps*₂₀₇₋₂ and *cps*_{K22} share three glycosyltransferases that can be related to the formation of the following glycosidic bonds: Gal(β1-4)Glcβ in the backbone, and Glc(α1-4)Galβ and GlcA(β1-

768
769 6)Glc α in the side chain (Fig. S5). The precise reaction catalyzed by each of these three GTs can be
770 inferred by comparison with other strains with which **CPS KK207-2** and K22 share only one
771 glycosidic bond and therefore, one GT in their gene clusters [5]. More precisely, they share the
772 Gal(β 1-4)Glc β structure and the WcuW GT with K25 [5,19], and the GlcA(β 1-6)Glc α structure and
773 the WckA GT with K23 [5,22]. By exclusion, WcmA GT, the third common GT between *cps*₂₀₇₋₂
774 and *cps*_{K22}, can be predicted to catalyze the addition of the first sugar residue of the side chain to the
775 backbone, Glc(α 1-4)Gal β (Fig. 7).
776
777
778
779

780 Two genes carried by the transposon insertion in *cps*₂₀₇₋₂ (*orf13* and *orf15*) code for GTs not
781 present in the *cps*_{K22} cluster, they can be predicted to catalyze the remaining two glycosidic bonds
782 in the side chain. In an attempt to identify the precise reaction catalyzed by these enzymes, it was
783 found that **CPS KK207-2** shares only one glycosidic bond with the K18 polysaccharide [5,21],
784 namely Glc(α 1-4)GlcA β (Fig. S5). Comparison of the protein sequences of the GTs coded in the
785 *cps* clusters of these two strains showed an acceptable homology level only between the protein
786 coded by *orf13* of *cps*_{K207-2} and WcuH of *cps*_{K18} (51% identities, 67% positives), strongly
787 suggesting that this GT is responsible for the addition of the activated α -D-Glcp residue to C4 of the
788 uronic acid. By exclusion, the GT coded by *orf15* should catalyze the addition of the terminal β -D-
789 Glcp residue to C6 of the α -D-Glcp in the side chain. This hypothesis was confirmed by comparison
790 with the K26 type [5,23], since the structure Glc(β 1-6)Glc α is common to both CPSs (Fig. S5).
791 Sequence analysis identified homology between the protein coded by *orf15* and the
792 glycosyltransferase WcuU (41% identities, 57% positives).
793
794
795
796
797
798
799
800

801 Despite the structural similarities of **CPS KK207-2** and K41 side chains (Glc(β 1-6)Glc(α 1-
802 4)GlcA(β)) which might explain the cross-reactivity observed for three ST258 *K. pneumoniae*
803 clinical strains isolated in a Greek hospital [25], comparison of the GTs coded by *cps*_{KK207-2} and
804 *cps*_{K41} did not retrieve any similarity. After comparison of common and unique genes and structures
805 of K41 and K12 antigens, Pan et al. [5] suggested that WcpT and WcpU might be the GTs involved
806 in the synthesis of the side chain of K41 CPS. Nevertheless, this seems unlikely for two reasons: i)
807 the *wcpT* and *wcpU* sequences are actually part of a unique gene in a *K. oxytoca* strain genome
808 (GenBank accession no. CP026285, locus_tag="C2U42_08200") and ii) in the *cps*_{K41} cluster the
809 *wcpT* and *wcpU* sequences flank an *IS1* transposase insertion which might have interrupted a single
810 gene sequence. Therefore, it is likely that some of the *cps*_{K41} genes have yet to be identified. The
811 biochemical pathway for the synthesis of the **CPS KK207-2** repeating unit is reported in Fig. 7 and
812 the data are summarized in Table 2.
813
814
815
816
817
818
819
820
821
822
823
824
825
826

827
828 **Author Contributions:**

829 P. C. and R. R. designed the study. B. B. purified the capsular polysaccharide, performed all the wet
830 chemistry experiments and GLC-MS analyses of carbohydrate derivatives, prepared figures. N. R.,
831 P. C., B. B. and R. R. recorded and interpreted NMR spectra. C. L. grew the bacteria and assigned
832 the glycosyltransferases functions. M. M. D. and G. M. R. contributed to genetic analysis. P. C., N.
833 R., and C. L. wrote the main manuscript text and prepared figures. All authors critically reviewed
834 and edited the manuscript.
835
836
837
838

839
840
841 **Competing interests**

842 Authors have no competing interests to declare.
843
844

845
846 **Acknowledgments**

847 Funding: This work was supported by the University of Trieste (FRA 2015).
848
849

850
851 **References**

- 852 [1] M.K. Paczosa, J. Meccas, *Klebsiella pneumoniae*: Going on the Offense with a Strong Defense,
853 Microbiol. Mol. Biol. Rev. 80(3) (2016) 629–661. <https://doi.org/10.1128/MMBR.00078-15>.
854
855 [2] C-R. Lee, J.H. Lee, K.S. Park, Y.B. Kim, B.C. Jeong, S.H. Lee, 2016. Global dissemination of
856 carbapenemase-producing *Klebsiella pneumoniae*: epidemiology, genetic context, treatment
857 options, and detection methods, Front. Microbiol. 7, 895.
858 <https://doi.org/10.3389/fmicb.2016.00895>.
859
860 [3] S. Brisse, V. Passet, A.B. Haugaard, A. Babosan, N. Kassis-Chikhani, C. Struve, D. Decré, *wzi*
861 gene sequencing, a rapid method for determination of capsular type for *Klebsiella* strains, J.
862 Clin. Microbiol. 51 (2013) 4073–4078. <https://doi.org/10.1128/JCM.01924-13>.
863
864 [4] Y.J. Pan, T.L. Lin, Y.H. Chen, C.R. Hsu, P.F. Hsieh, M.C. Wu, J.T. Wang, 2013. Capsular
865 types of *Klebsiella pneumoniae* revisited by *wzc* sequencing, PLoS ONE 8(12), e80670.
866 <https://doi.org/10.1371/journal.pone.0080670>.
867
868 [5] Y.J. Pan, T.L. Lin, C.T. Chen, Y.Y. Chen, P.F. Hsieh, C.R. Hsu, M.C. Wu, J.T. Wang, 2015.
869 Genetic analysis of capsular polysaccharide synthesis gene clusters in 79 capsular types of
870 *Klebsiella* spp., Scientific Reports 5, 15573. <https://doi.org/10.1038/srep15573>.
871
872 [6] M.M. D'Andrea, F. Amisano, T. Giani, V. Conte, N. Ciacci, S. Ambretti, L. Santoriello, G.M.
873 Rossolini, 2014. Diversity of capsular polysaccharide gene clusters in Kpc-producing
874 *Klebsiella pneumoniae* clinical isolates of sequence type 258 involved in the italian epidemic,
875 PLoS ONE 9(5), e96827. <https://doi.org/10.1371/journal.pone.0096827>.
876
877
878
879
880
881
882
883
884
885

- 886
887
888
889
890
891
892
893
894
895
896
897
898
899
900
901
902
903
904
905
906
907
908
909
910
911
912
913
914
915
916
917
918
919
920
921
922
923
924
925
926
927
928
929
930
931
932
933
934
935
936
937
938
939
940
941
942
943
944
- [7] F.R. Deleo, L. Chen, S.F. Porcella, C.A. Martens, S.D. Kobayashi, A.R. Porter, K.D. Chavda, M.R. Jacobs, B. Mathema, R.J. Olsen, R.A. Bonomo, J.M. Musser, B.N. Kreiswirth, Molecular dissection of the evolution of carbapenem-resistant multilocus sequence type 258 *Klebsiella pneumoniae*, Proc. Natl. Acad. Sci. 111(13) (2014) 4988–4993. <https://doi.org/10.1073/pnas.1321364111>.
- [8] P. Albersheim, D.J. Nevins, P.D. English, A. Karr, A method for the analysis of sugars in plant cell-wall polysaccharides by gas-liquid chromatography, Carbohydr. Res. 5 (1967) 340–345. [https://doi.org/10.1016/S0008-6215\(00\)80510-8](https://doi.org/10.1016/S0008-6215(00)80510-8).
- [9] K. Kakehi, S. Honda, Silyl ethers of carbohydrates, in: C.J. Biermann, G.D. McGinnis (Eds.), Analysis of carbohydrates by GLC and MS, Boca Raton (FL), CRC Press, 1989, pp. 43–85.
- [10] P.J. Harris, R.J. Henry, A.B. Blakeney, B.A. Stone, An improved procedure for the methylation analysis of oligosaccharides and polysaccharides, Carbohydr. Res. 127 (1984) 59–73. [https://doi.org/10.1016/0008-6215\(84\)85106-X](https://doi.org/10.1016/0008-6215(84)85106-X).
- [11] D.P. Sweet, R.H. Shapiro, P. Albersheim, Quantitative analysis by various g.l.c. response-factor theories for partially methylated and partially ethylated alditol acetates, Carbohydr. Res. 40 (1975) 217–225. [https://doi.org/10.1016/S0008-6215\(00\)82604-X](https://doi.org/10.1016/S0008-6215(00)82604-X).
- [12] R.L. Taylor, H.E. Conrad, Stoichiometric depolymerization of polyuronides and glycosaminoglycuronans to monosaccharides following reduction of their carbodiimide-activated carboxyl group, Biochemistry 11 (1972) 1383–1388. <https://doi.org/10.1021/bi00758a009>.
- [13] S.F. Osman, W.F. Fett, M.L. Fishman, Exopolysaccharides of the phytopathogen *Pseudomonas syringae* pv. Glycinea, J. Bacteriol. 166(1) (1986) 66–71. <https://doi.org/10.1128/jb.166.1.66-71.1986>.
- [14] G.J. Gerwig, J.P. Kamerling, J.F.G. Vliegthart, Determination of the d and l configuration of neutral monosaccharides by high-resolution capillary g.l.c., Carbohydr. Res. 62 (1978) 349–357. [https://doi.org/10.1016/S0008-6215\(00\)80881-2](https://doi.org/10.1016/S0008-6215(00)80881-2).
- [15] I.J. Goldstein, G.W. Hay, B.A. Lewis, F. Smith, Controlled degradation of polysaccharides by periodate oxidation, reduction, and hydrolysis, Methods Carbohydr. Chem. 5, (1965) 361–370.
- [16] J.M. Lau, M. McNeil, A.G. Darvill, P. Albersheim, Selective degradation of the glycosyluronic acid residues of complex carbohydrates by lithium dissolved in ethylenediamine, Carbohydr. Res. 168 (1987) 219–243. [https://doi.org/10.1016/0008-6215\(87\)80028-9](https://doi.org/10.1016/0008-6215(87)80028-9).
- [17] P.E. Jansson, L. Kenne, G. Widmalm, Computer-assisted structural analysis of polysaccharides with an extended version of CASPER using ¹H- and ¹³C-NMR data. Carbohydr. Res. 188 (1989) 169–191. [https://doi.org/10.1016/0008-6215\(89\)84069-8](https://doi.org/10.1016/0008-6215(89)84069-8).

- 945
946 [18] L.A. Parolis, H. Parolis, H. Niemann, S. Stirm, Primary structure of *Klebsiella* serotype K22
947 capsular polysaccharide: another glycan containing 4-O-[(S)-1-carboxyethyl]-D-glucuronic
948 acid, Carbohydr. Res. 179 (1988) 301–314. [https://doi.org/10.1016/0008-6215\(88\)84126-0](https://doi.org/10.1016/0008-6215(88)84126-0).
949
950 [19] H. Niemann, B. Kwiatkowski, U. Westphal, S. Stirm, *Klebsiella* serotype 25 capsular
951 polysaccharide: primary structure and depolymerization by a bacteriophage-borne glycanase, J.
952 Bacteriol. 130 (1977) 366–374.
953
954 [20] B. Lindberg, B. Lindqvist, J. Lönngren, W. Nimmich, Structural studies of the capsular
955 polysaccharide of *Klebsiella* type 37, Carbohydr. Res. 58 (1977) 443–451.
956 [https://doi.org/10.1016/S0008-6215\(00\)84371-2](https://doi.org/10.1016/S0008-6215(00)84371-2).
957
958 [21] G.G.S. Dutton, K.L. Mackie, M.T. Yang, Structural investigation of *Klebsiella* serotype K18
959 polysaccharide, Carbohydr. Res. 65 (1978) 251–263. [https://doi.org/10.1016/S0008-](https://doi.org/10.1016/S0008-6215(00)84317-7)
960 [6215\(00\)84317-7](https://doi.org/10.1016/S0008-6215(00)84317-7).
961
962 [22] G.G.S. Dutton, K.L. Mackie, A.V. Savage, M.D. Stephenson, Structural investigation of the
963 capsular polysaccharide of *Klebsiella* serotype K23, Carbohydr. Res. 66, (1978) 125–131.
964 [https://doi.org/10.1016/S0008-6215\(00\)83245-0](https://doi.org/10.1016/S0008-6215(00)83245-0).
965
966 [23] J. Di Fabio, G.G.S. Dutton, Structural investigation of the capsular polysaccharide of *Klebsiella*
967 serotype K26, Carbohydr. Res. 92, (1981) 287–298. [https://doi.org/10.1016/S0008-](https://doi.org/10.1016/S0008-6215(00)80399-7)
968 [6215\(00\)80399-7](https://doi.org/10.1016/S0008-6215(00)80399-7).
969
970 [24] J.P. Joseleau, M. Lapeyre, M. Vignon, G.G.S. Dutton, Chemical and n.m.r.-spectroscopic
971 investigation of the capsular polysaccharide of *Klebsiella* serotype K41, Carbohydr. Res. 67
972 (1978) 197–212. [https://doi.org/10.1016/S0008-6215\(00\)83742-8](https://doi.org/10.1016/S0008-6215(00)83742-8).
973
974 [25] L.S. Tzouveleakis, V. Miriagou, S.D. Kotsakis, K. Spyridopoulou, E. Athanasiou, E. Karagouni,
975 E. Tzelepi, G.L. Daikos, KPC-producing, multidrug-resistant *Klebsiella pneumoniae* sequence
976 type 258 as a typical opportunistic pathogen, Antimicrob. Agents Chemother. 57 (2013) 5144–
977 5146. <https://doi.org/10.1128/AAC.01052-13>.
978
979
980
981
982
983
984
985
986
987
988

989 Appendix

990 Supplementary material
991
992
993
994
995
996
997
998
999
1000
1001
1002
1003

Table 1

¹H and ¹³C chemical shift assignments of **CPS deOAc-KK207-2**. Spectra were recorded at 600 MHz at 343 K.

Residue	Chemical shifts (ppm) ^a					
	H-1 C-1	H-2 C-2	H-3 C-3	H-4 C-4	H-5 C-5	H-6 C-6
→6)-α-D-Glcp-(1→ (A)	5.48 98.9	3.52 72.5	3.72 73.7	3.52 70.0	3.87 71.8	3.90, 4.11 68.7
→6)-α-D-Glcp-(1→ (B)	4.92 99.5	3.52 72.6	3.78 73.4	3.69 69.7	4.32 71.2	3.95, 4.10 68.5
→4)-β-D-Glcp-(1→ (C)	4.69 105.1	3.25 74.2	3.66 75.5	3.50 80.9	3.58 75.7	3.77, 4.00 61.7
→3,4)-β-D-Galp-(1→ (D)	4.59 103.8	3.74 71.7	3.92 82.0	4.27 76.2	3.88 76.5	~3.86 61.0
β-D-Glcp-(1→ (E)	4.49 103.5	3.34 74.0	3.52 76.6	3.42 70.6	3.46 76.7	3.74, 3.91 61.7
→6)-β-D-GlcpA-(1→ (F)	4.48 103.3	3.42 73.9	3.78 77.1	3.80 77.4	3.80 77.5	175.4

^a Chemical shifts are given relative to acetone (2.225 ppm for ¹H and 31.07 ppm for ¹³C).

1063
1064
1065
1066
1067
1068
1069
1070
1071
1072
1073
1074
1075
1076
1077
1078
1079
1080
1081
1082
1083
1084
1085
1086
1087
1088
1089
1090
1091
1092
1093
1094
1095
1096
1097
1098
1099
1100
1101
1102
1103
1104
1105
1106
1107
1108
1109
1110
1111
1112
1113
1114
1115
1116
1117
1118
1119
1120
1121

Table 2

Assignments of glycosyltransferases (GT) catalysed reactions on the basis of CPS structural homology and protein sequence homology.

GT	Glycosidic bond	Accession no.	K type	Reference	
				Structure	<i>cps</i> cluster
WcuW	β -D-Galp(1→4)- β -D-Glcp	BAT23470.1	K25	[19]	[5]
		BA027504.1	K22	[18]	[5]
		BAT23694.1	K37	[20]	[5]
		CCI88053.1	KK207-2	This work	[6]
WcmA	α -D-Glcp(1→4)- β -D-Galp	BA027502.1	K22	[18]	[5]
		BAT23692.1	K37	[20]	[5]
		CCI88051.1	KK207-2	This work	[6]
WckA	β -D-GlcpA(1→6)- α -D-Glcp	BAT23435.1	K23	[22]	[5]
		BA027503.1	K22	[18]	[5]
		BAT23693.1	K37	[20]	[5]
		CCI88052.1	KK207-2	This work	[6]
WcuH	α -D-Glcp(1→4)- β -D-GlcpA	BAT23379.1	K18	[21]	[5]
		CCI88056.1	KK207-2	This work	[6]
WcuU	β -D-Glcp(1→6)- α -D-Glcp	BAT23487.1	K26	[23]	[5]
		CCI88058.1	KK207-2	This work	[6]

1122
1123 **FIGURE LEGEND**
1124

1125 **Fig. 1.** ¹H NMR spectra of **PH-2** (a), **SD-2** (b), **SD-1** (c), **de-OAc CPS KK207-2** (d), **Li CPS**
1126 **KK207-2** (e).
1127

1128
1129 **Fig. 2.** ESI mass spectrum of the oligosaccharide **SD-2** (a) and ESI MS² of the ion at 483.2 *m/z* (b);
1130 ESI mass spectrum of the oligosaccharide **SD-1** (c) and ESI MS² of the ion at 615.1 *m/z* (d).
1131
1132 Assignments are indicated in the figures.
1133

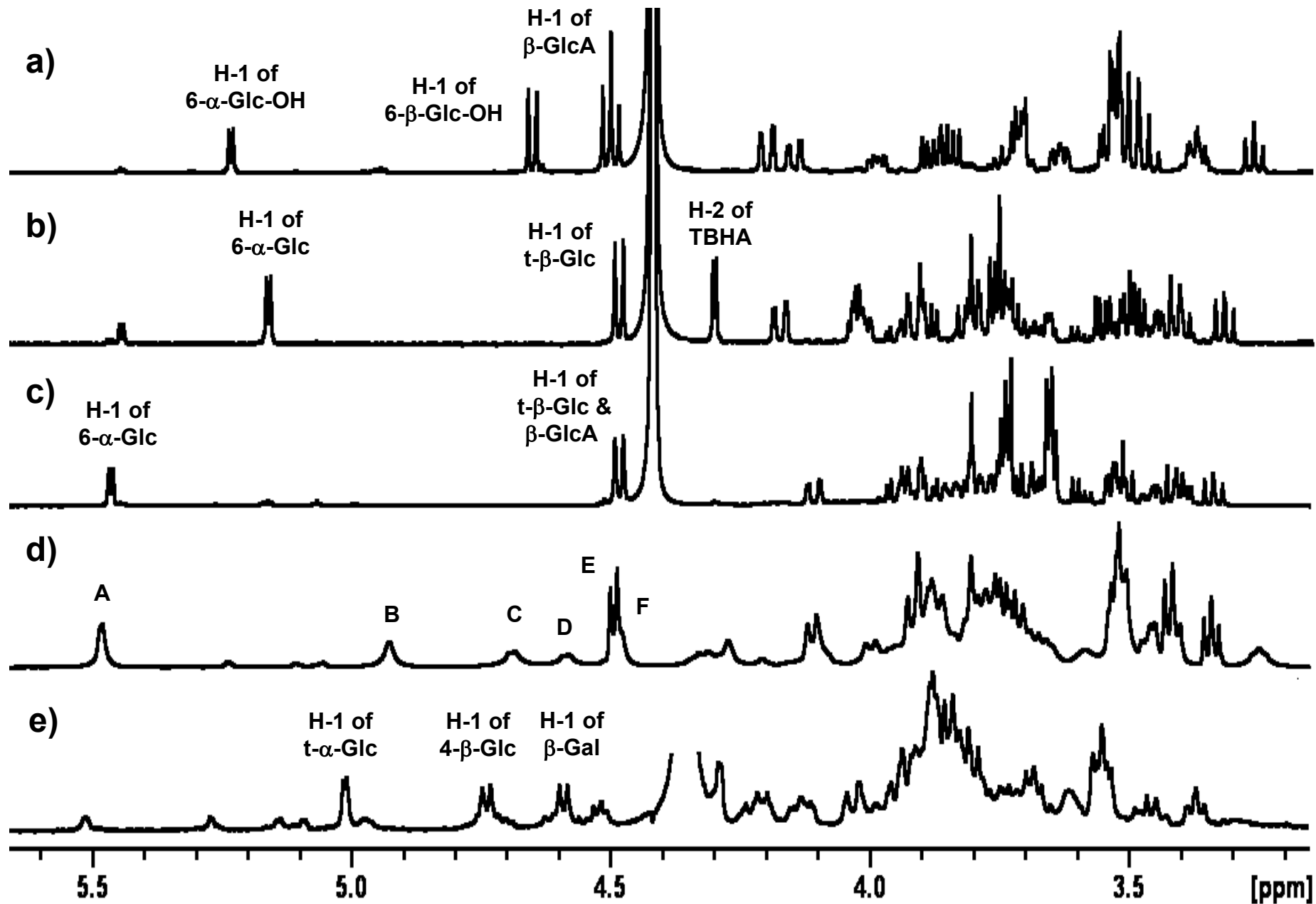
1134
1135 **Fig. 3.** Overlay of the COSY (red)/TOCSY (black) anomeric region of **deOAc CPS KK207-2**
1136 recorded at 600 MHz and 343K. The insert shows crosspeaks for residues **B**, **C** and **D** present at a
1137 lower level. Crosspeaks have been labelled according to the corresponding residue (**A** to **E**).
1138

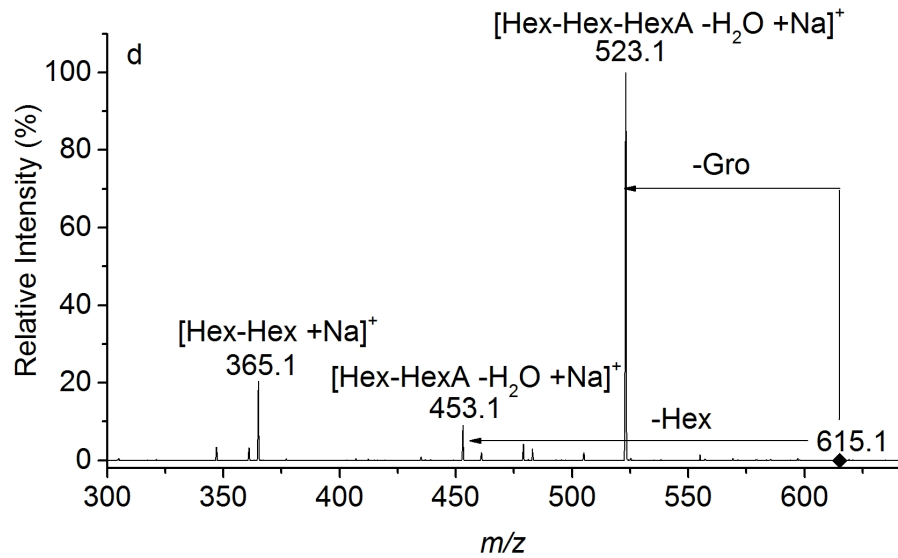
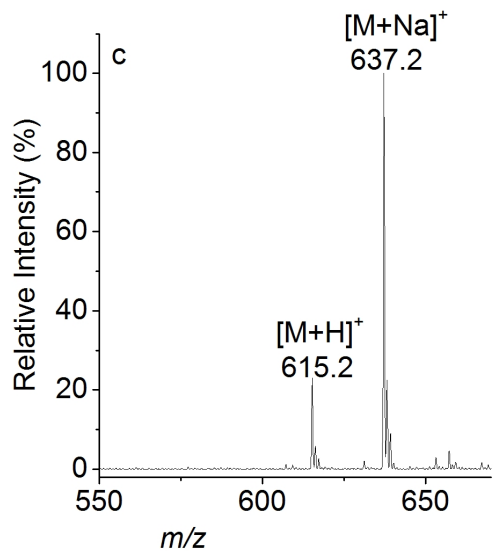
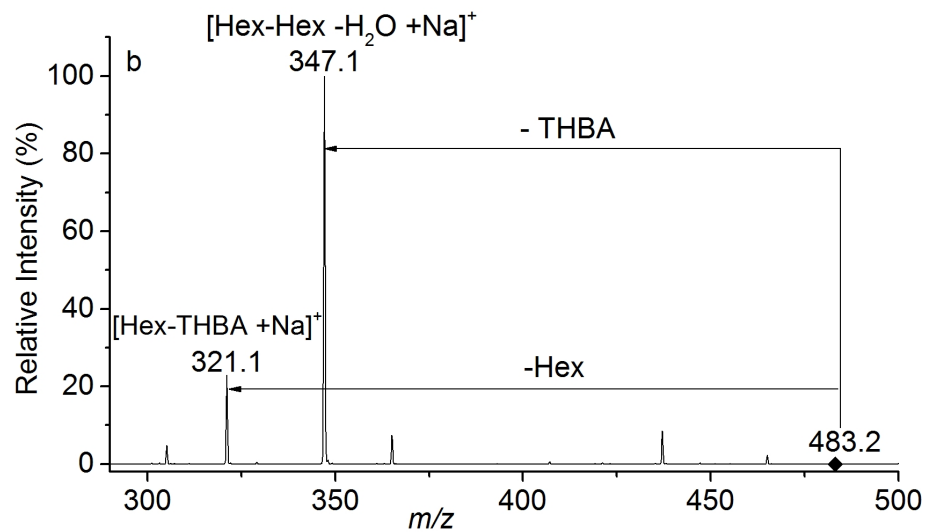
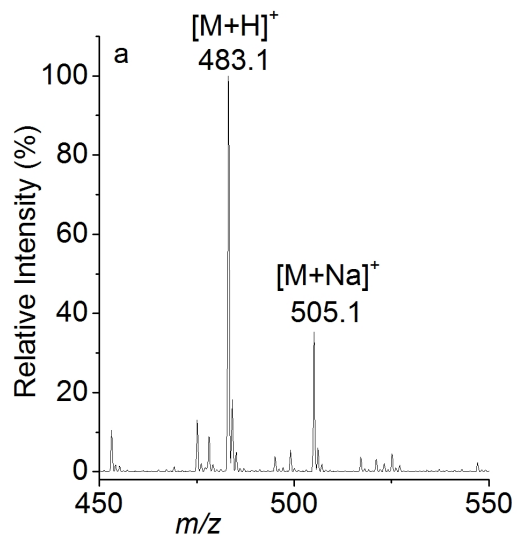
1139
1140 **Fig. 4.** Expansion of the NOESY anomeric region of **deOAc CPS KK207-2** recorded at 600 MHz
1141 and 343K. Intra- and inter-residue correlation crosspeaks have been labelled according to the
1142 corresponding residue (**A** to **E**).
1143

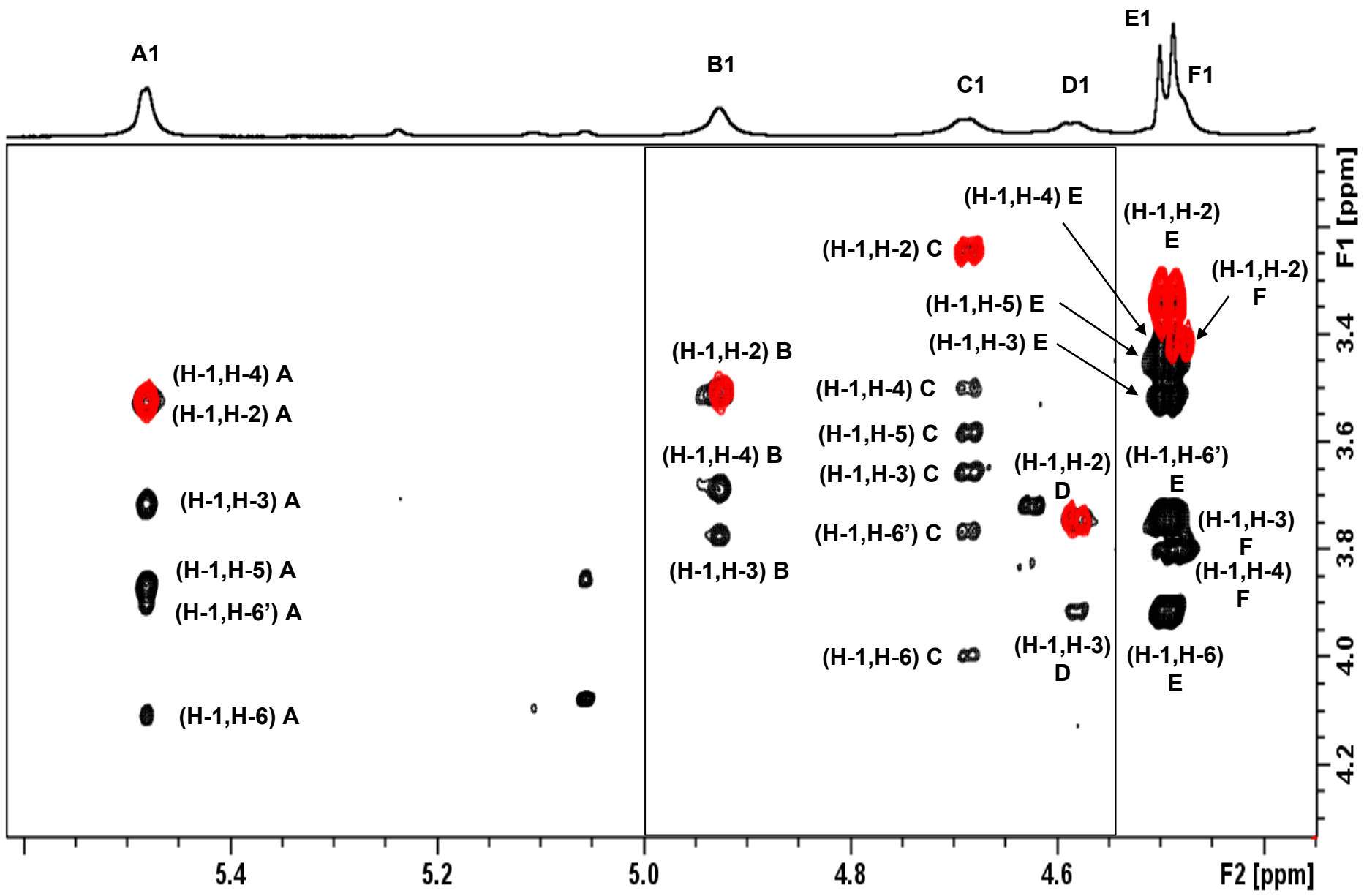
1144
1145 **Fig. 5.** Expansion of the 1D ¹³C NMR spectrum of **deOAc CPS KK207-2** recorded at 150 MHz
1146 and 343K showing the anomeric and ring regions. Carbon peaks have been labelled according to the
1147 corresponding residue (**A** to **E**). Methylene assignments were confirmed by recording the DEPT
1148 spectrum.
1149

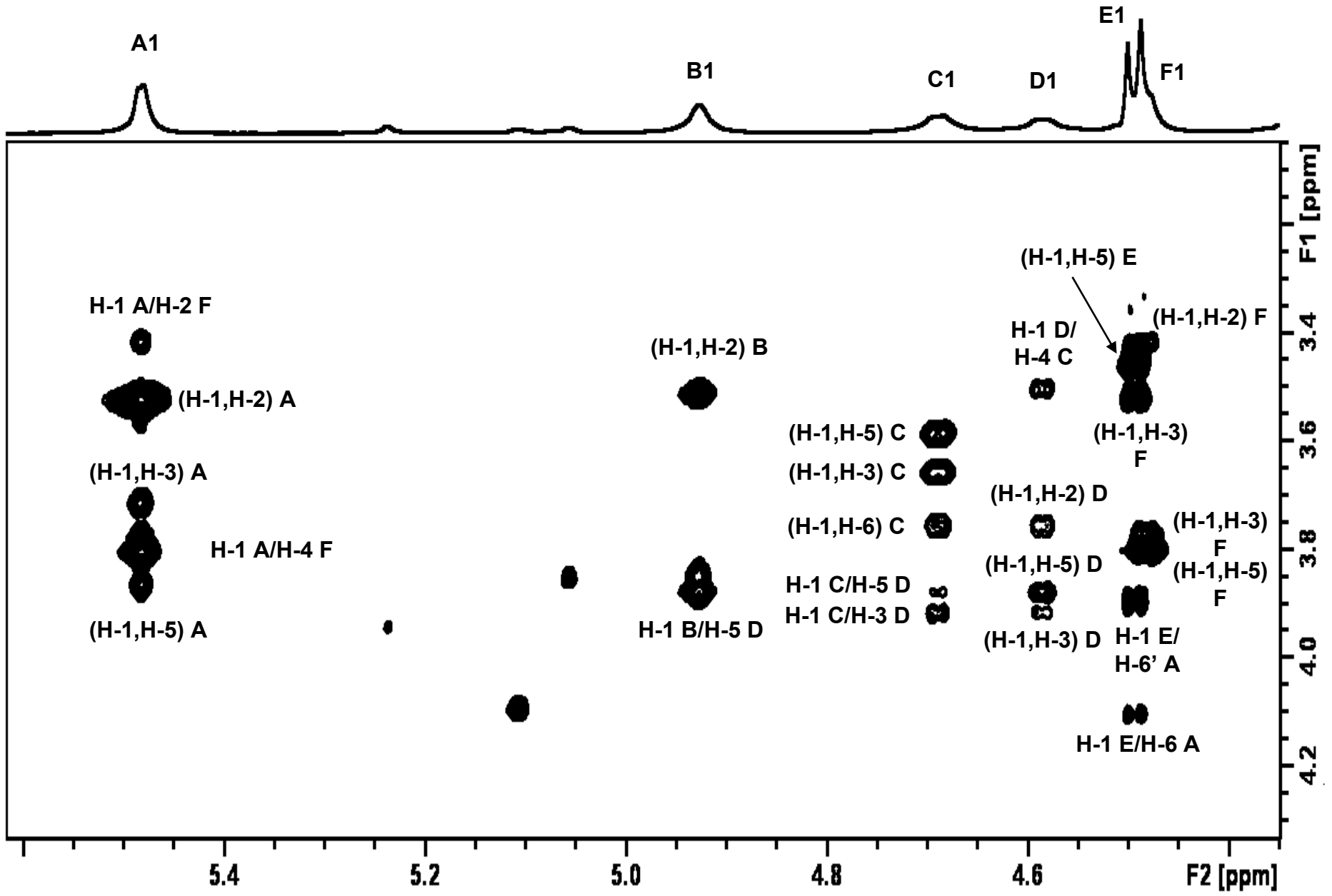
1150
1151 **Fig. 6.** Expansion overlay of the HSQC (red)/HMBC (black) spectra of **deOAc CPS KK207-2**
1152 recorded at 600 MHz and 343K. The corresponding parts of the ¹H (1D DOSY) and ¹³C NMR
1153 spectra are shown along the horizontal and vertical axis, respectively. Proton/carbon crosspeaks
1154 have been labelled according to the corresponding residue (**A** to **E**).
1155

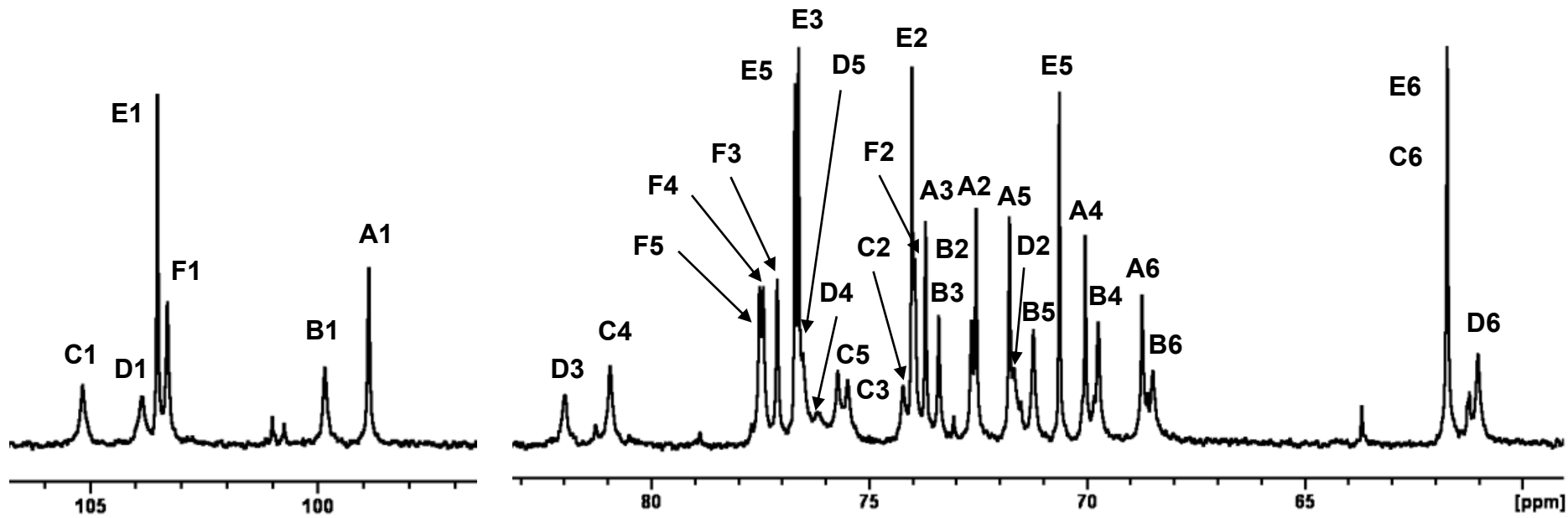
1156
1157 **Fig. 7.** Proposed glycosyltransferase and polymerase activity of the *Klebsiella pneumoniae* KK207-
1158 **2 cps** gene cluster. Glycosyltransferases responsible for each elongation step are listed above the
1159 respective glycosidic linkage. The polymerization site is marked by an arrow (a). Identification of
1160 genes coded in the central region of the *cps*₂₀₇₋₂ cluster (portion 8294-19716 of accession number
1161 HE866752). *ISEcII*-like and a truncated version of *ISI*-like insertion sequences are indicated by a
1162 blue and a green box, respectively (b).
1163
1164
1165
1166
1167
1168
1169
1170
1171
1172
1173
1174
1175
1176
1177
1178
1179
1180

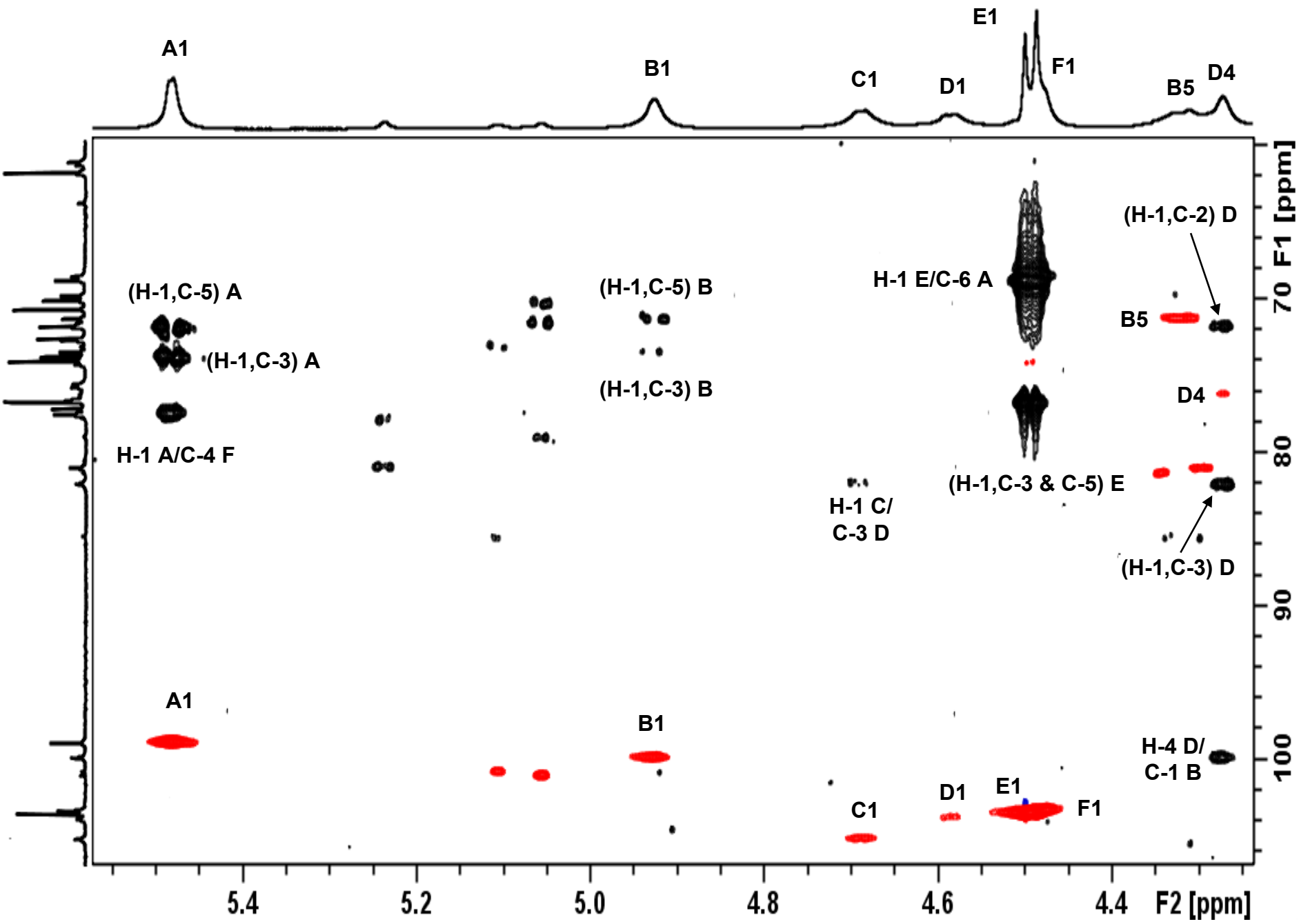


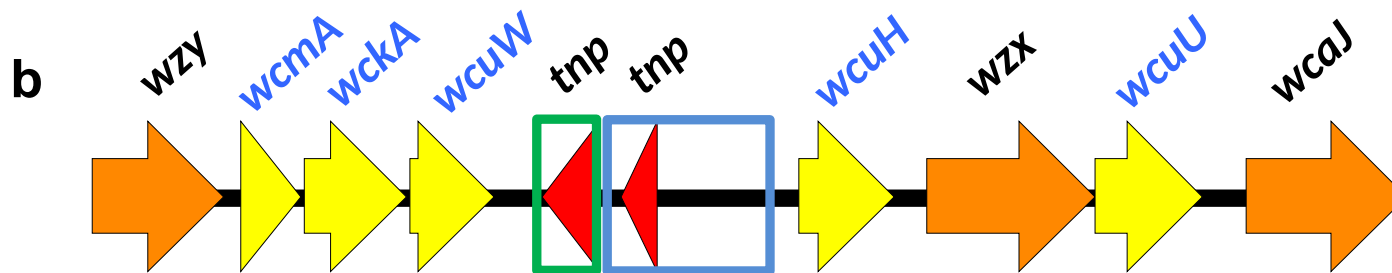
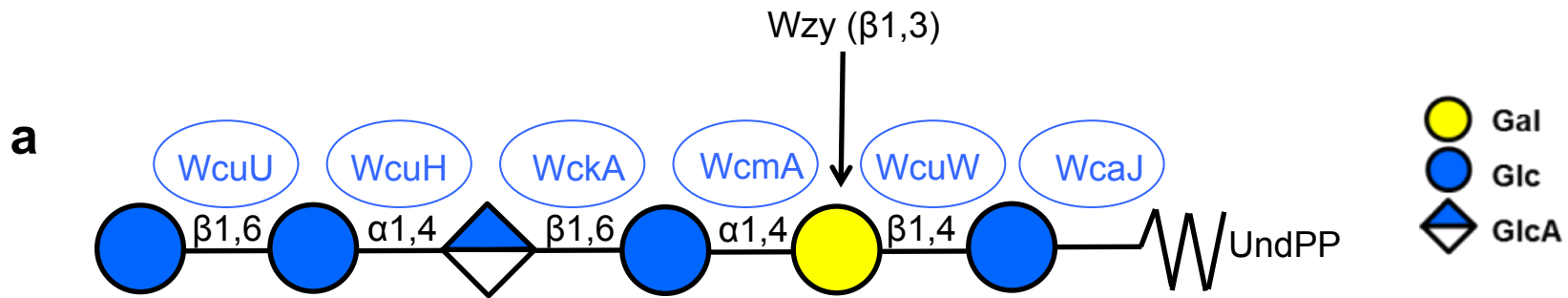












SUPPLEMENTARY MATERIAL

Structure of the capsular polysaccharide of the KPC-2-producing *Klebsiella pneumoniae* strain KK207-2 and assignment of the glycosyltransferases functions

Barbara Bellich^a, Neil Ravenscroft^b, Roberto Rizzo^a, Cristina Lagatolla^a, Marco Maria D'Andrea^{c,d}
Gian Maria Rossolini^{e,f} and Paola Cescutti^{a*}

^a Department of Life Sciences, University of Trieste, via L. Giorgieri 1, Bdg C11, 34127 Trieste, Italy

^b Department of Chemistry, University of Cape Town, Rondebosch 7701, South Africa

^c Department of Medical Biotechnologies, University of Siena, Siena, Italy

^d Department of Biology, University of Rome "Tor Vergata", Rome, Italy

^e Department of Experimental and Clinical Medicine, University of Florence, Florence, Italy

^f Microbiology and Virology Unit, Florence Careggi University Hospital, Florence, Italy

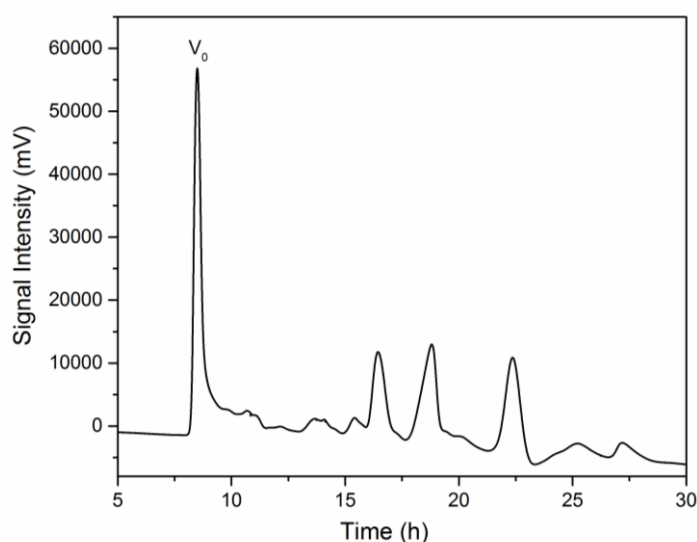


Fig. S1: Bio Gel P2 elution profile of the products obtained after lithium degradation of the **CPS-KK207-2**. Fraction eluting in the void volume of the column (V_0 peak) were pooled, named **Li CPS KK207-2**, and used for recording NMR spectra.

Table S1

Determination of the glycosidic linkages in **CPS KK207-2** native and after carboxyl reduction, and **SD-Vo** by GLC-MS of PMAA derivatives.

Linkage ^a	Relative molar ratio ^c				
	RRT ^b	I	II	III	IV
t-Glc	1.00	1.00	1.00	1.00	0.41
4-Glc	1.22	1.00	1.98	2.85	1.18
3-Gal	1.23	-	-	1.07	0.44
6-Glc	1.26	1.64	1.92	0.67	0.28
3,4-Gal	1.34	1.12	1.44	1.35	0.56

^a t-Glc= terminal non-reducing glucose; the numbers indicate the position of the glycosidic linkages, e.g. 4-Glc = 4-linked glucose; ^b Relative retention time; ^c Peak areas were corrected by the effective carbon response factor [11] and the molar ratio are expressed relative to t-Glc in columns I, II, III and to the sum of 3-Gal + 3,4-Gal in column IV; I = native **CPS KK207-2**; II = **CPS KK207-2** after -COOH reduction [12,13]; III = **SD-Vo**; IV = **SD-Vo** with molar ratios relative to the sum of 3-Gal + 3,4-Gal.

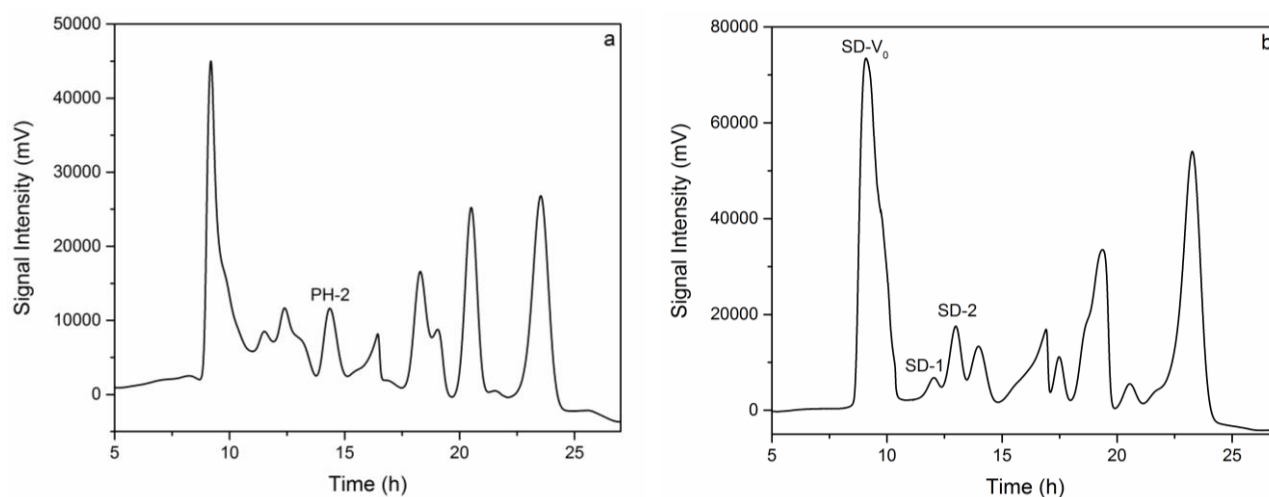


Fig. S2: Bio Gel P2 elution profiles of the products obtained after partial hydrolysis (a) and Smith degradation (b) of **deOAc CPS KK207-2**. Labeled peaks contained mainly only one oligosaccharide and were subjected to ESI-MS and ¹H NMR spectroscopy analyses.

Table S2

¹H and ¹³C chemical shift assignments of the sample **SD-2** obtained from Smith degradation of the **CPS KK207-2**. Spectra were recorded at 500 MHz and 333 K.

Residue	Chemical shifts (ppm) ^a					
	H-1 C-1	H-2 C-2	H-3 C-3	H-4 C-4	H-5 C-5	H-6 C-6
→6)-α-D-Glcp-(1→	5.15	3.54	3.76	3.49	4.00	3.87, 4.16
	99.83	72.66	73.89	70.51	72.06	69.59
β-D-Glcp-(1→	4.48	3.31	3.49	3.40	3.44	3.73, 3.91
	103.65	74.02	76.67	70.59	76.76	61.73
→3)-2,3,4 trihydroxy-butanoic acid	-	4.29	4.02	3.79, 3.76		
	-	74.21	82.24	61.51		

^aChemical shifts are given relative to internal acetone (2.225 ppm for ¹H and 31.07 ppm for ¹³C).

Table S3

¹H and ¹³C chemical shift assignments of the sample **SD-1** obtained from Smith degradation of the **CPS KK207-2**. Spectra were recorded at 500 MHz and 333 K.

Residue	Chemical shifts (ppm) ^a					
	H-1 C-1	H-2 C-2	H-3 C-3	H-4 C-4	H-5 C-5	H-6 C-6
→6)-α-D-Glcp-(1→	5.47	3.53	3.71	3.53	3.85	3.89 4.11
	99.11	72.63	73.68	70.09	71.83	68.80
β-D-Glcp-(1→	4.49	3.34	3.51	3.41	3.45	3.74 3.92
	103.57	74.02	76.70	70.66	76.74	61.78
→4)-β-D-GlcpA-(1→	4.49	3.40	3.78	3.81	3.81	-
	103.57	74.02	77.16	77.65	77.65	
→1)-Gro	3.95 3.67	3.85	3.66 3.61			
	71.93	71.83	63.44			

^aChemical shifts are given relative to internal acetone (2.225 ppm for ¹H and 31.07 ppm for ¹³C).

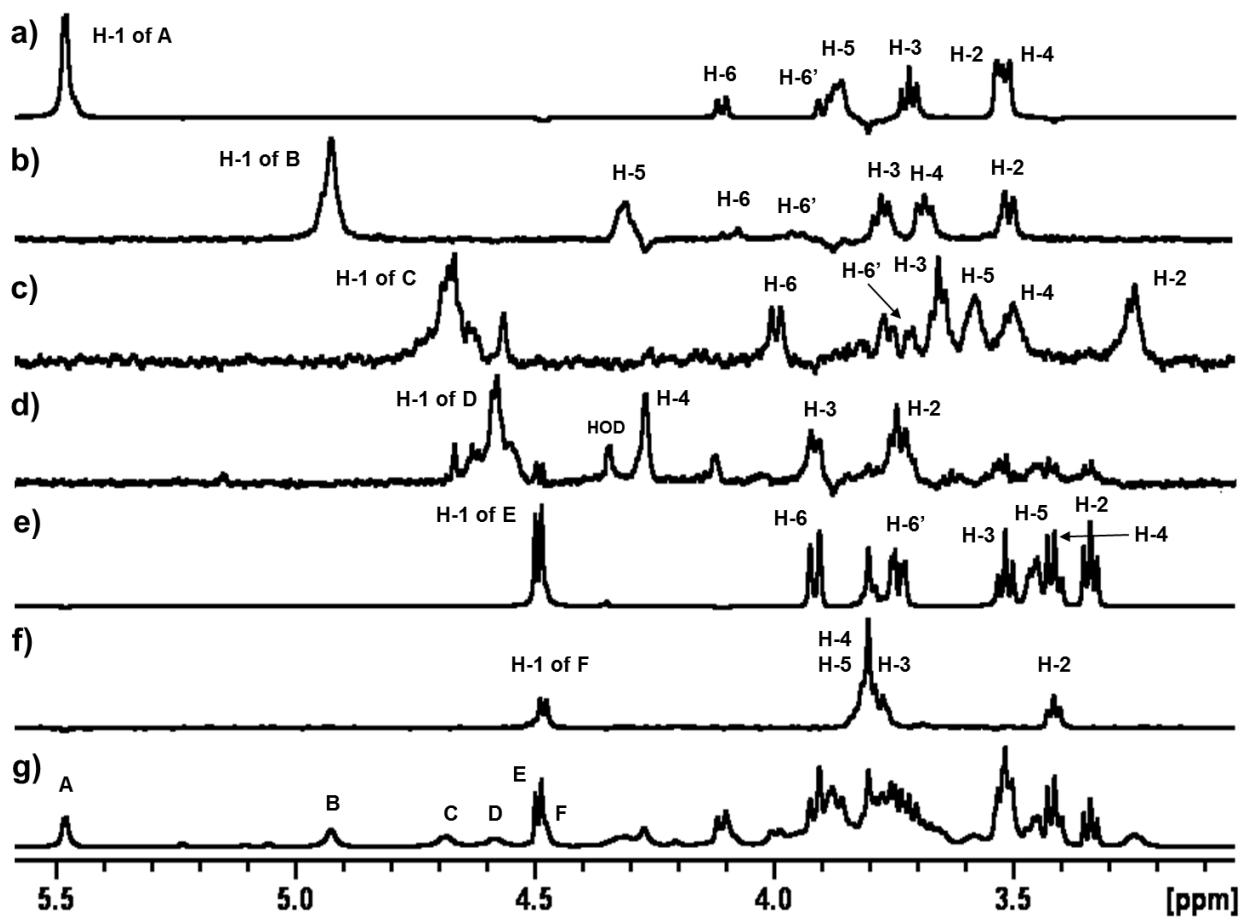


Fig. S3: ^1H NMR spectra of deOAc CPS KK207-2. Selective 1D TOCSY experiments performed by irradiation of the anomeric protons for residues A to F (a to f) overlaid with the ^1D DOSY spectrum of the CPS (g). Spectra were recorded at 600 MHz and 343 K using a mixing time of 200 ms.

Table S4

^1H and ^{13}C chemical shift assignments of the **Li CPS KK207-2** obtained from Lithium degradation [16] of the **CPS KK207-2**. Spectra were recorded at 600 MHz and 343 K.

Residue	Chemical shifts (ppm) ^a					
	H-1 C-1	H-2 C-2	H-3 C-3	H-4 C-4	H-5 C-5	H-6 C-6
$\alpha\text{-D-Glcp-(1}\rightarrow$	4.98	3.52	3.78	3.52	4.18	~3.84
	100.20	72.74	73.53	70.26	72.45	61.21
$\rightarrow\text{4)-}\beta\text{-D-Glcp-(1}\rightarrow$	4.71	3.34	3.66	3.64	3.56	3.83, 4.00
	105.13	74.17	75.42	80.16	75.66	61.33
$\rightarrow\text{3,4)-}\beta\text{-D-Galp-(1}\rightarrow$	4.56	3.79	3.87	4.26	3.81	-
	103.96	71.63	81.62	76.63	76.56	

^aChemical shifts are given relative to internal acetone (2.225 ppm for ^1H and 31.07 ppm for ^{13}C).

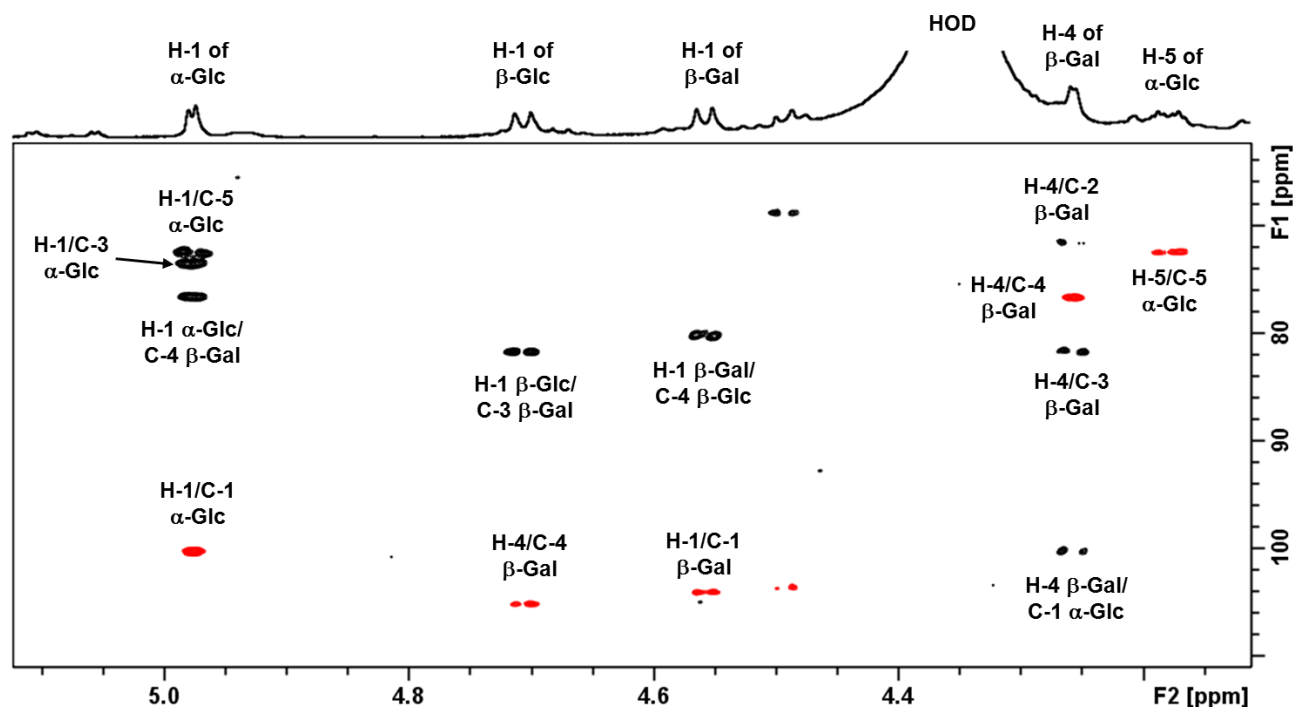


Fig. S4: Expansion overlay of the HSQC (red)/HMBC (black) spectra of **Li CPS KK207-2** recorded at 600 MHz and 343K. The proton/carbon crosspeaks have been labelled according to the corresponding residue ($\alpha\text{-Glc}$, $\beta\text{-Glc}$ and $\beta\text{-Gal}$); the small peaks are due to residual $\beta\text{-GlcA}$. The inter-residue correlations confirm the linkages and sequence: $\alpha\text{-D-Glc-(1}\rightarrow\text{4)-}\beta\text{-D-Gal-(1}\rightarrow$ and the disaccharide backbone, $\rightarrow\text{4)-}\beta\text{-D-Glc-(1}\rightarrow\text{3)-}\beta\text{-D-Gal-(1}\rightarrow$.

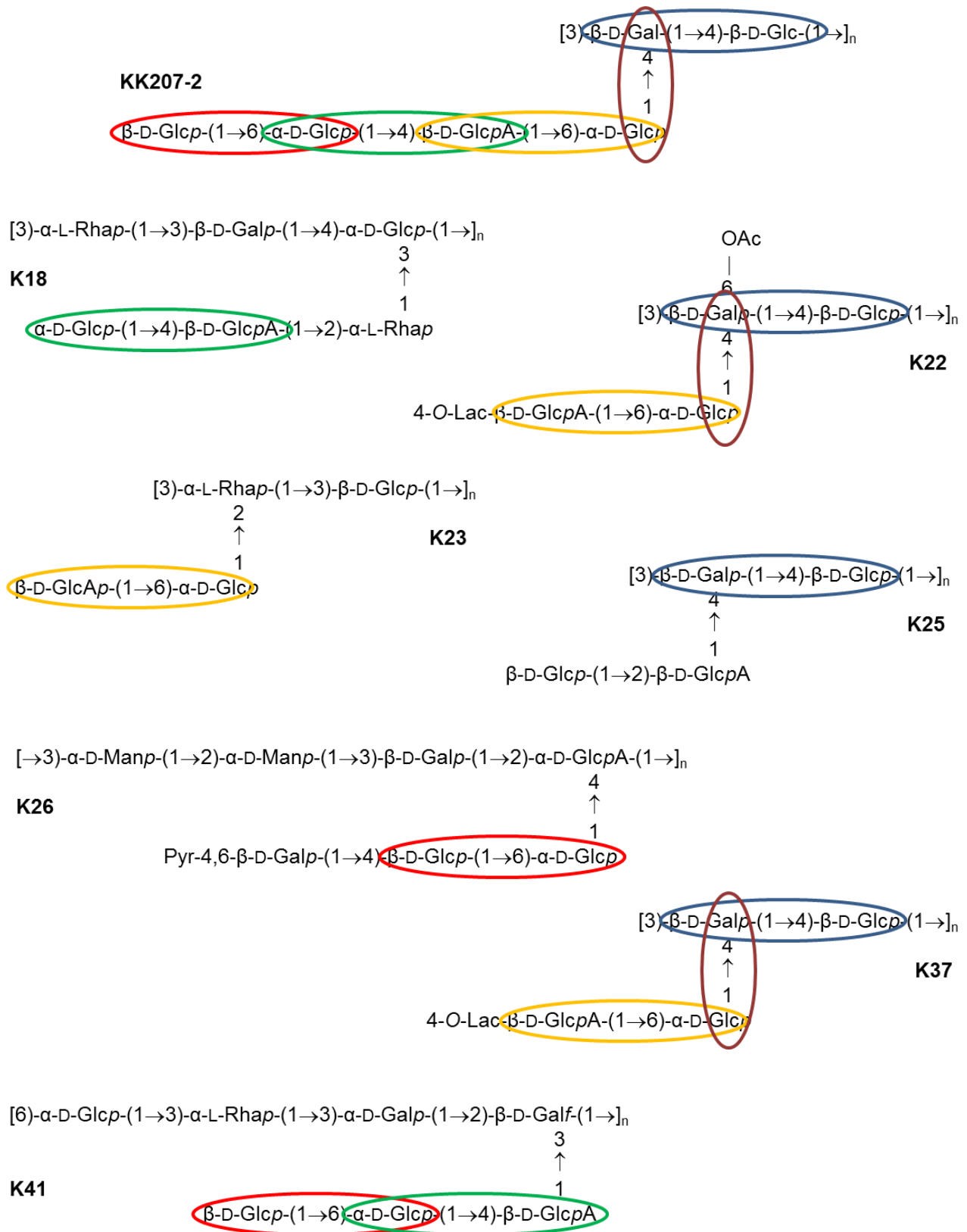


Fig. S5: Structure of the repeating units of different CPS: **KK207-2** (this article), K18 [21], K22 [18], K23 [22], K25 [19], K26 [23], K37 [20] and K41 [24] *Klebsiella pneumoniae* capsular polysaccharides. Circles of different colours highlight common glycosidic linkages. These structural similarities were used to assign the corresponding GTs genes.